iScience

CellPress
OPEN ACCESS

Article

# African Arowana Genome Provides Insights on Ancient Teleost Evolution

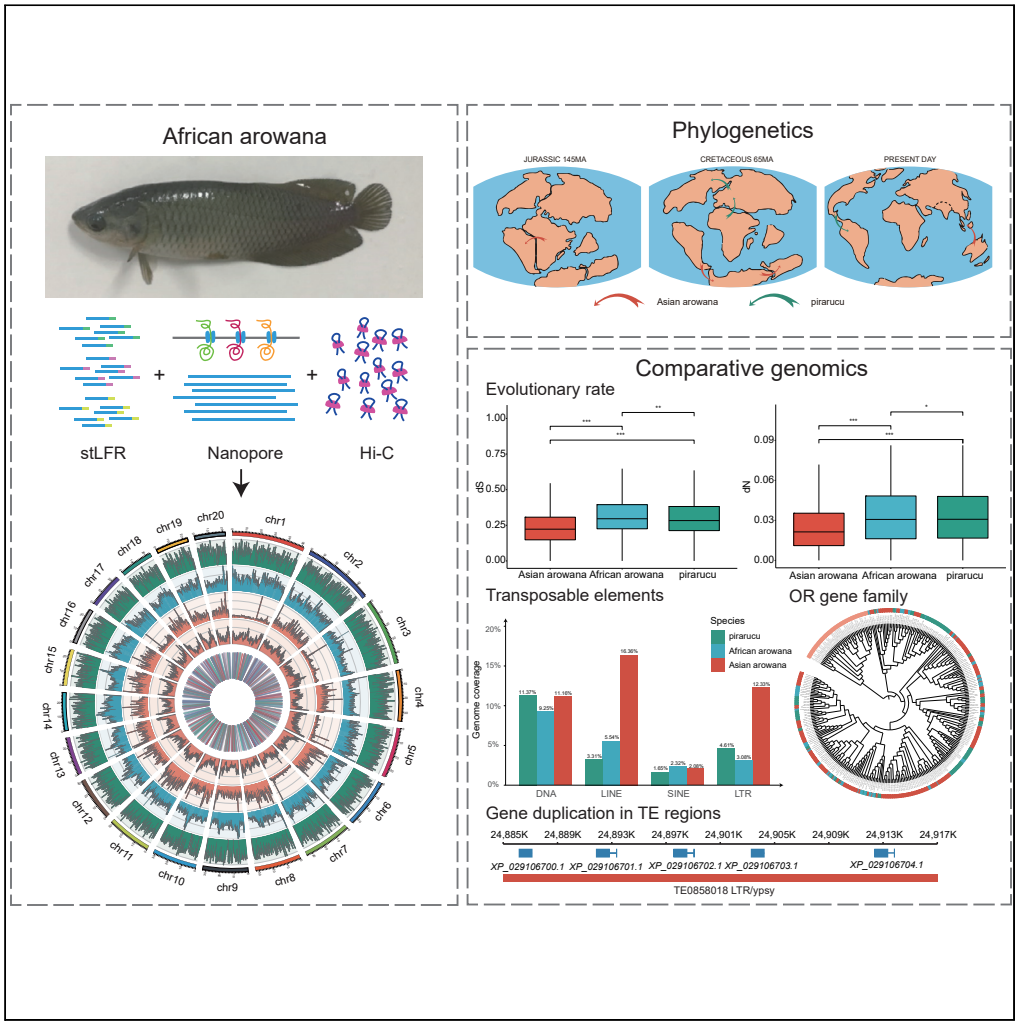


Shijie Hao, Kai Han, Lingfeng Meng, ..., Xun Xu, Xin Liu, Guangyi Fan

liuxin@genomics.cn (X.L.)
fanguangyi@genomics.cn (G.F.)

## HIGHLIGHTS

An evolutionary model of *Osteoglossidae* along the continental drift is provided

A faster evolving rate of African arowana than Asian arowana is revealed

The gene duplications of Asian arowana are related to more class I TE insertions

A mechanism of African arowana's feeding habits transition is proposed.

Hao et al., iScience *23*, 101662
November 20, 2020 
https://doi.org/10.1016/j.isci.2020.101662

iScience

CellPress
OPEN ACCESS

Article

# African Arowana Genome Provides Insights on Ancient Teleost Evolution

Shijie Hao,[1,2,9] Kai Han,[2,9] Lingfeng Meng,[1,2] Xiaoyun Huang,[2] Wei Cao,[3] Chengcheng Shi,[1,2] Mengqi Zhang,[2] Yilin Wang,[2] Qun Liu,[2] Yaolei Zhang,[2,5] Haixi Sun,[3] Inge Seim,[6,7] Xun Xu,[2,3,8] Xin Liu,[2,3,4,*] and Guangyi Fan[2,3,4,10,*]

## SUMMARY

***Osteoglossiformes* is a basal clade of teleost, evolving since the Jurassic period. The genomes of *Osteoglossiformes* species would shed light on the evolution and adaptation of teleost. Here, we established a chromosome-level genome of African arowana. Together with the genomes of pirarucu and Asian arowana, we found that they diverged at ~106.1 million years ago (MYA) and ~59.2 MYA, respectively, which are coincident with continental separation. Interestingly, we identified a dynamic genome evolution characterized by a fast evolutionary rate and a high pseudogenization rate in African arowana and pirarucu. Additionally, more transposable elements were found in Asian arowana which confer more gene duplications. Moreover, we found the contraction of olfactory receptor and the expansion of UGT in African arowana might be related to its transformation from carnivore to be omnivore. Taken together, we provided valuable genomic resource of *Osteoglossidae* and revealed the correlation of biogeography and teleost evolution.**

## INTRODUCTION

*Osteoglossiformes* is an ancient group of teleosts, which comprises five living groups including *Hiodontidae*, *Osteoglossidae*, *Pantodontidae*, *Notopteridae* and *Mormyridae*. *Osteoglossidae* contains two clades of *Osteoglossinae* and *Heterotidinae*, with species distributing in Asia, America, Africa, and Australia (Wilson and Murray, 2008). The existence of *Osteoglossiformes* can be dated back to the Jurassic period according to fossil evidences (Lavoue and Sullivan, 2004; Wilson and Murray, 2008), thus current species in *Osteoglossiformes* should had witnessed the break-up of the Gondwana supercontinent (Cioffi et al., 2019; Kumazawa and Nishida, 2000; Lavoue, 2016). Therefore, *Osteoglossiformes* species, serving as models for biogeography, have been extensively studied in morphological and molecular evolution (Hilton, 2001, 2003; Kumazawa and Nishida, 2000; Lavoue and Sullivan, 2004; TANG et al., 2004), and also provide evidences for paleogeology. Previous efforts have been made to decode genomes of *Osteoglossiformes* species (Bian et al., 2016; Du et al., 2019; Gallant et al., 2017), while more whole-genome sequences, especially those with chromosome information and comprehensive genome comparisons, which would further illustrate the evolutionary process of *Osteoglossiformes*.

African arowana (or African bonytongue, *Heterotis niloticus*), pirarucu (*Arapaima gigas*), and Asian arowana (*Scleropages formosus*) are three representative species of *Osteoglossidae* in *Osteoglossiformes* with some morphological differences (Adite et al., 2017; Axelrod et al., 1986; saint-Paul, 1986). African arowana is the only omnivore in *Osteoglossiformes* (Adite et al., 2013; Oliveira et al., 2019), distributing majorly in Africa, compared to pirarucu mainly in South America and Asian arowana in Southeast Asia. Despite their differences in habitats and morphology, these three species are relatively closely related with similar behaviors and physiological characters (Monentcham et al., 2009; Núñez et al., 2011; Scott and Fuller, 1976), making them good representative species for investigating the genetic basis of the ancient teleost clade (Betancur et al., 2017). In this study, we assembled the genome of African arowana using advanced sequencing and library-building technologies. In addition, together with the available genome sequences of Asian arowana and pirarucu, we comprehensively analyzed the genome evolution of *Osteoglossiformes* and illustrated the evolutionary features of *Osteoglossiformes*.

[1]BGI Education Center, University of Chinese Academic of Sciences, Shenzhen 518083, China

[2]BGI-Qingqao, BGI-Shenzhen, Qingdao, 266555, China

[3]BGI-Shenzhen, Shenzhen 518083, China

[4]State Key Laboratory of Agricultural Genomics, BGI-Shenzhen, Shenzhen 518083, China

[5]Department of Biotechnology and Biomedicine, Technical University of Denmark, Lyngby, 2800, Denmark

[6]Integrative Biology Laboratory, College of Life Sciences, Nanjing Normal University, Nanjing, 210046, China

[7]School of Biology and Environmental Science, Queensland University of Technology, Brisbane 4102, QLD, Australia

[8]Guangdong Provincial Key Laboratory of Genome Read and Write, BGI-Shenzhen, Shenzhen 518120, China

[9]These authors contributed equally

[10]Lead Contact

*Correspondence: liuxin@genomics.cn (X.L.), fanguangyi@genomics.cn (G.F.)

https://doi.org/10.1016/j.isci.2020.101662

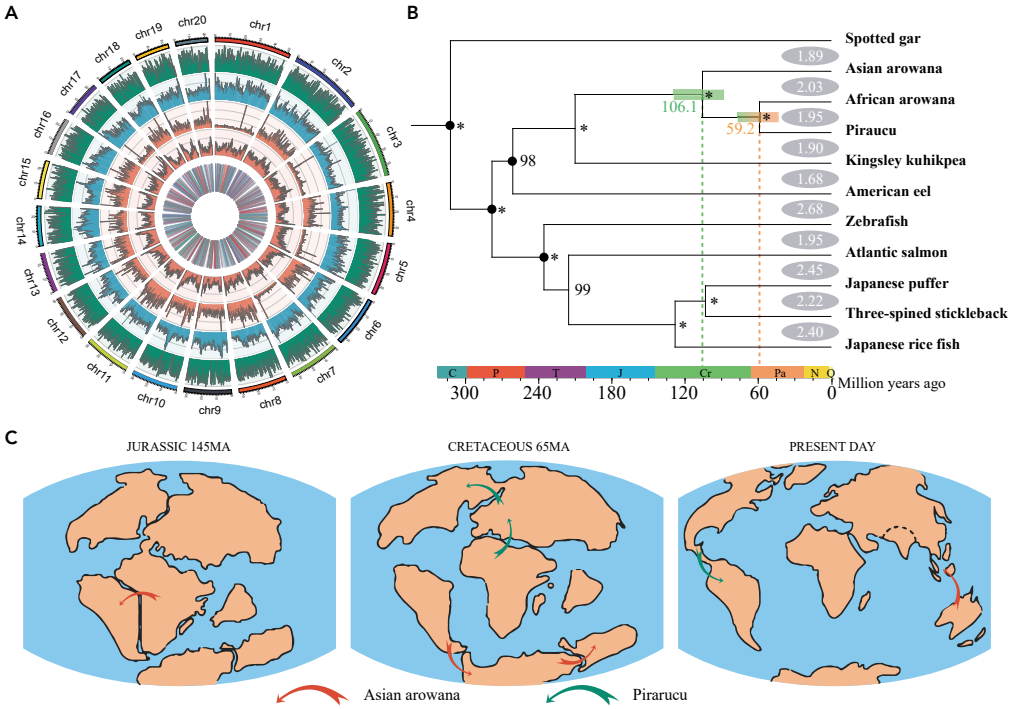


**Figure 1. The Evolution History of Asian arowana, African arowana and Pirarucu**

(A) The characteristics of the assembled *H. niloticus* genome. The tracks from outer to inner represent the gene density, TE density, tandem repeat density, GC content and non-coding RNA respectively.

(B) The phylogenetic relationships of 10 teleost fishes with *L. oculatus* as outgroup. The numbers on clades represent the evolutionary rates (dN + dS). The numbers beside the inner nodes represent the support values of the nodes (The asterisk represents a support value of 100).

(C) pirarucu and Asian arowana' divergence pattern through the continents drift.

## RESULTS

### Sequencing and Assembly of a Chromosome-Level African Arowana Genome

In order to sequence and assemble the African arowana genome, we applied single tube long fragment read (stLFR) technology (Wang et al., 2018) on BGISEQ-500 sequencing platform and generated 144.36 Gb (~186×) data (Table S1). In total, ~669.7 Mb (~99% of the estimated genome size, 673.41Mb, Figure S1) genomic sequences were assembled with a scaffold N50 of ~9.62 Mb. To further improve the continuity, we sequenced ~10.2 Gb (~13.1×) Nanopore long reads to fill the gaps. With these long reads, the contig N50 was further improved from 255.6 Kb to 2.31 Mb (Table S2) using TGS-GapCloser (Xu et al., 2019). To anchor the scaffold sequences to chromosomes, we constructed a Hi-C library and sequenced ~21.2 Gb Hi-C data and thus ~650.44 Mb sequences were anchored to 20 chromosomes (Figures 1A, S2, and Table S3), which was consistent with the previous report on African arowana karyotype (Oliveira et al., 2019). The complete African arowana mitochondria genome was assembled using MitoZ (Meng et al., 2019), and it was almost identical to the published African arowana mitochondrial genome (Figure S3), thus indicating the correctness of sampling and species identification. Finally, by using BUSCO (Benchmarking Universal Single-Copy Orthologs) (Simao et al., 2015), we found that ~97.6% of the complete vertebrate BUSCO genes were covered by our assembly(Table S4), providing further evidence for the fine quality of the assembled genome.

We then carried out genome annotation to identify repeats and protein-coding genes of African arowana. About 18.74% of this genome was annotated and identified as "repetitive sequences", and DNA transposable elements (TEs) are the most abundant. We also predicted 24,146 protein-coding genes with combinational annotation methods (*de novo* prediction, homology-based prediction and RNA-seq-based prediction) in this genome (Table S3), of which ~89.5% were found to have homologs in public databases (Kyoto Encyclopedia of Genes and Genomes, Swiss-Prot, Translated EMBL, NCBI non-redundant proteins) with known functions (Table S5). Clustering with 10 other fishes, we identified 15,432 gene families in African arowana, of which 30 are unique to African arowana.

### Speciation of *Osteoglossiformes* along with the Geographic Drift

To validate and add to the previously proposed model of Gondwana origin and plate tectonic transportation of *Osteoglossiformes* species (Kumazawa and Nishida, 2000), we constructed the phylogenetic tree of the representative species in *Osteoglossiformes*. Collecting the ten teleost species (African arowana, Asian arowana, pirarucu, American eel (*Anguilla rostrate*), Atlantic salmon (*Salmo salar*), Kingsley kuhikpea (*Paramormyrops kingsleyae*), Japanese puffer (*Takifugu rubripes*), Japanese rice fish (*Oryzias latipes*), three-spined stickleback (*Gasterosteus aculeatus*), Zebrafish (*Danio rerio*)) with available genome sequences and spotted gar (*Lepisosteus oculatus*) as an outgroup species, we identified 355 single-copy gene families (one orthologous gene in each species) and then used them to build the phylogenetic tree, reflecting the relationship and evolution of teleost (Figure 1B). The divergence time of each internal node was calculated using MCMCTree (Yang, 2007) with the calibration of previous molecular or fossil researches obtained from TimeTree (http://www.timetree.org/, Table S6). In this phylogenetic tree, the divergence time between Asian arowana and the common ancestor of African arowana and pirarucu was ~106.1 million years ago (MYA), which was moderate to previous researches (Cioffi et al., 2019; Du et al., 2019; Vialle et al., 2018). And the divergence time estimated here was close to the final separation time of South American and African continents in Afro-South American drift of Gondwana supercontinent happened at ~110 MYA (Rogers and Santosh, 2004). Considering the previous evidences supporting that (1) *Osteoglossinae* fishes speciated along with the separation of South America, Antarctic, Australia, and Southeast Asia from ~50.3MYA (Cioffi et al., 2019); (2) Presently, Asian arowana only lives in Southeast Asia (Mu et al., 2012); and (3) Africa has been identified as the taxonomic diversity center of *Osteoglossiformes* (Wilson and Murray, 2008), we proposed that the ancestor of Asian arowana had migrated from Africa to Southeast Asia before or during the tectonic-mediated Gondwanan fragmentation (especially the fragmentation of Africa-South America, South America-Antarctica-Australia and the fragmentation of Southeast Asia-Australia) (Figure 1C). Then, the divergence time between African arowana and pirarucu was estimated as ~59.2 MYA (Figure 1B), which was also close to the split time of North American and Eurasian continents (~65 MYA or later) (Rafferty, 2010; Rogers and Santosh, 2004). Additionally, a Paleocene (56–65Ma) *Heterotidinae* fossil was discovered in North America (Guo-Qing and Wilson, 1996) and classified as an outgroup of African arowana and pirarucu (Wilson and Murray, 2008). Thus, we concluded that the ancestor of African arowana and pirarucu might live in both North America and Eurasia continents of Gondwana supercontinent, and after the split of these continents, the two species have evolved separately, while pirarucu had spread to South America after the formation of Isthmus of Panama (Figure 1C). Hence, by using the whole-genome data analysis, we proposed the association between the speciation of *Osteoglossiformes* species and the paleo-geographical changes and improved the previous model for speciation of these species.

### Main Distinct Genomic Evolution Events of Three *Osteoglossidae* Fishes during Their Adaptations to New Environments

#### *Dynamic Evolution Rate*

In addition to phylogenetic analysis, we further investigated these three genomes in detail to reveal the genome evolution during the long period after speciation. First, we calculated the dN and dS (the substitution rates at non-synonymous and synonymous sites) of 355 single-copy gene families in each clade. Comparing to the common ancestor, we found that the dN and dS values of Asian arowana (average dN: 0.024; average dS: 0.253) were lower than those of African arowana (average dN: 0.032; average dS: 0.317) and pirarucu (average dN: 0.032; average dS 0.307), indicating higher mutation rate and faster evolution in African arowana and pirarucu compared to Asian arowana (Figure 1B). In order to further validate these results, we identified 7,699 single-copy gene families among three *Osteoglossidae* fishes and spotted gar. For these orthologous gene families, we calculated the average dN and dS of these three *Osteoglossidae* species and also found that the dN and dS of African arowana (average dN: 0.039; average dS: 0.335) and pirarucu (average dN: 0.040; average dS: 0.346) were significantly greater than those of Asian arowana (average dN: 0.027; average dS: 0.242). The Wilcoxon rank-sum test showed that the differences between Asian arowana and either African arowana or pirarucu were statistically significant ($p$-value<0.05, Figure 2A). Besides, we investigated the number of pseudogenes (the remains of malfunctional genes because of mutation accumulation) of these three *Osteoglossidae* species and found more pseudogenes in African arowana (350) and pirarucu (399) than in Asian arowana (242).

We also explored the evolution rate of these three *Osteoglossidae* species' conserved regions. Whole-genome alignments of these three *Osteoglossidae* species were implemented firstly with spotted gar as

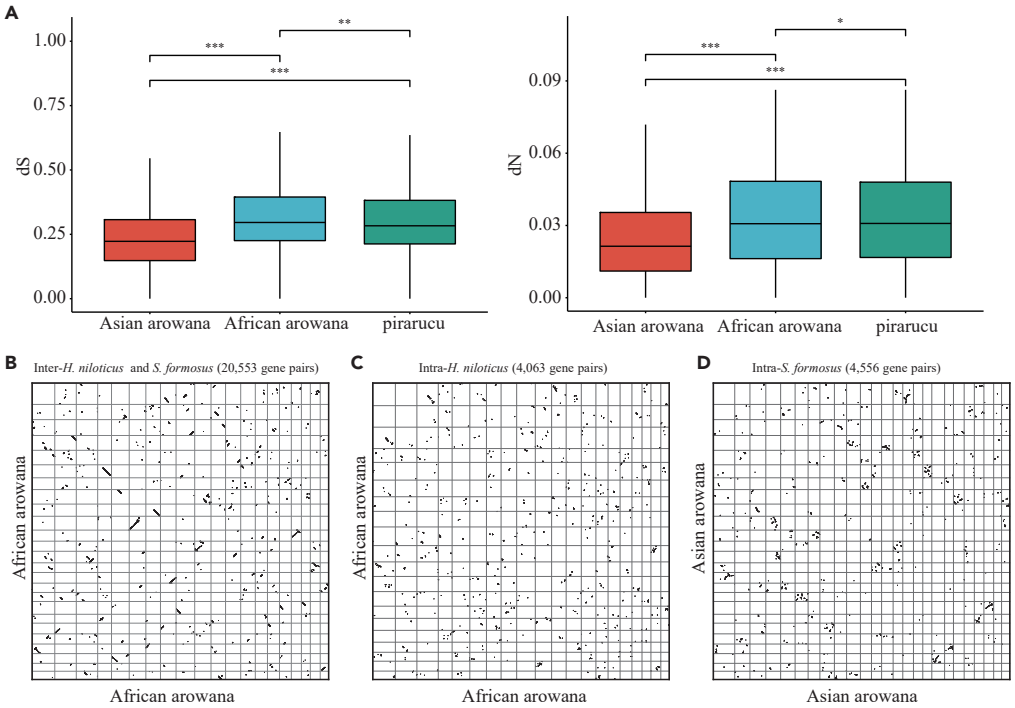


**Figure 2. The Evolution Rate of Asian arowana, African arowana and Pirarucu**

(A) The dS and dN distribution of Asian arowana, African arowana, and pirarucu. The statistic significancy was calculated by Wilcoxon rank-sum test and three asterisks indicate a p value that less than 2.22*e−16 and two asterisks indicate a p value that equal to $2.5 \times 10^{-11}$ while one asterisks indicate a p value that equal to 0.9.

(B) Syntenic pattern of African arowana and Asian arowana.

(C) Syntenic pattern of intra-African arowana.

(D) Syntenic pattern of intra-Asian arowana.

a reference. Then, we calculated the genetic distance (TN93 model) in the resulting 30 Mb conserved regions (remain in four species) between each *Osteoglossidae* species and spotted gar, respectively. And this analysis revealed that the average distance of African arowana (0.358) was significantly larger than Asian arowana (0.353) and pirarucu (0.351) (Wilcoxon rank-sum test, p value<$2.22 \times 10^{-16}$, Figure S4). Moreover, we identified syntenic blocks of African arowana and Asian arowana to further investigate the evolution of their genomes. We found a distinct colinear relationship between African arowana and Asian arowana, indicating slight chromosomal structural variations occurred between their genomes (Figure 2B). We also found a rough chromosomal one-to-one colinear relationship in Asian arowana itself, whereas more scattered self-syntenic blocks were detected in African arowana genome than in Asian arowana (Figures 2C and 2D). These results provided additional evidences supporting the faster evolution rate of African arowana, which had resulted in more variations in the paralogous chromosomes inheriting from the TS-WGD events (~350 MYA) (Glasauer and Neuhauss, 2014).

### *Extra Class I TE Insertion in Asian Arowana*

Other than the faster evolution rate in African arowana and pirarucu genomes, the genome sizes of these two species (669 Mb and 667 Mb, respectively) are also notably smaller than that of the Asian arowana genome (785 Mb). Thus, we then investigated the possible mechanisms underlying the smaller genome sizes. Performing the same combinational annotation methods (*de novo*- and homology-based methods), we annotated the TEs in all three *Osteoglossidae* fishes. Looking into the repeat content, we found it was substantially less in African arowana and pirarucu genomes (18.7% and 18.2%, respectively) than in Asian arowana genome (29.5%). The extra insertion in repeat content (~100 Mb) may explain the differences of genome sizes (Table S7). Further investigating the different categories of TEs, we found the LINEs (long interspersed nucleotide elements) and LTRs (long terminal repeats) proportions were notably different among African arowana (LINEs: 5.54%, 37.10 Mb and LTRs: 3.08%, 20.63 Mb), pirarucu (LINEs: 3.31%, 22.11 Mb and LTRs: 4.61%, 30.74 Mb) and Asian arowana (LINEs: 16.36%, 128.34 Mb and LTRs:

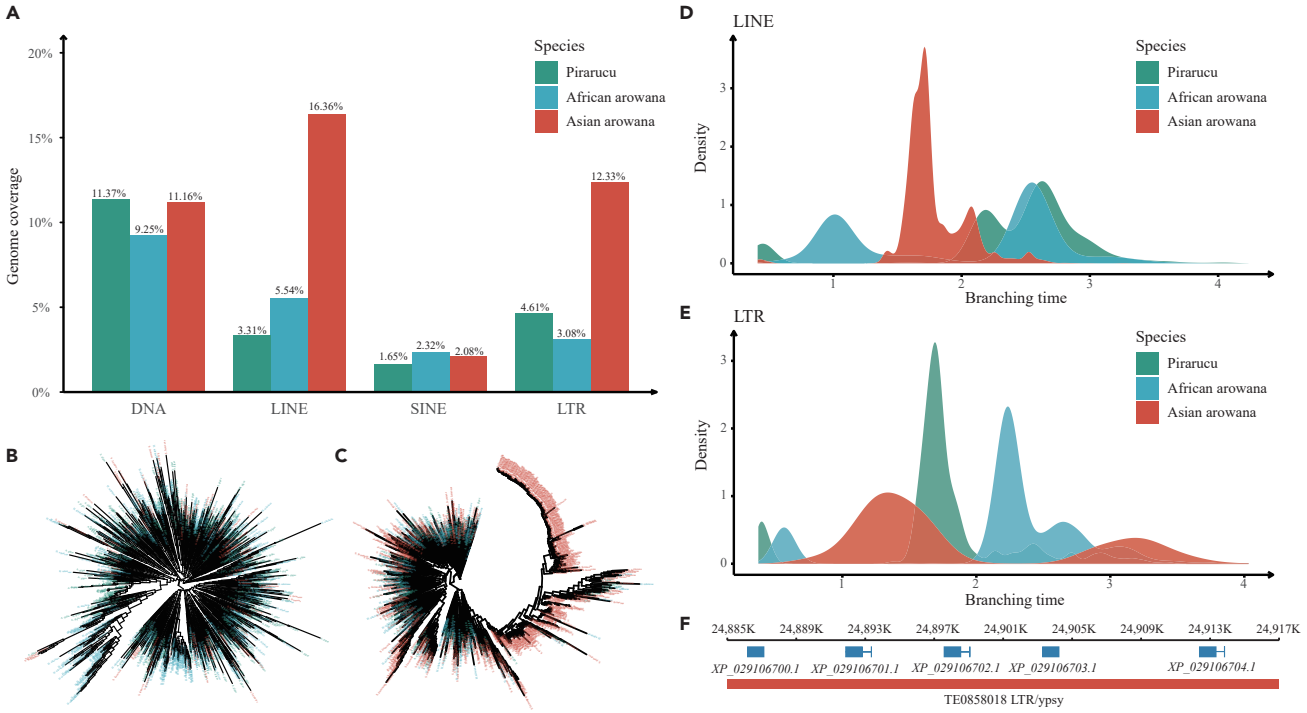


**Figure 3. Transposable Element (TE) Dynamics of Pirarucu, African Arowana and Asian Arowana**

(A) The distribution of three *Osteoglossidae* fishes' TEs.

(B) The phylogenetic trees of three *Osteoglossidae* fishes' Tc1 TEs.

(C) The phylogenetic trees of three *Osteoglossidae* fishes' Tigger TEs.

(D) The insertion timeline of LINE TEs of three *Osteoglossidae* fishes.

(E) The insertion timeline of LTR TEs of three *Osteoglossidae* fishes.

(F) An example of the positional relationship of Asian arowana's genes and TEs, in which the blue bars indicate the genes and the red bar indicate the TEs. In this case, all of the five genes are olfactory receptors.

12.33%, 96.77 Mb) (Figure 3A). Although, DNA TE proportions were comparable in 3 species, the most abundant DNA TE class of Asian arowana was TcMar-Tigger while TcMar-Tc1 was the most abundant in both African arowana and pirarucu, and the distinctly expanded clade of TcMar-Tigger of Asian arowana indicated a recent fast insertion event (Figures 3B and 3C).

Additionally, we estimated the relative insertion time of LINEs and LTRs through the Ty3 reverse transcriptase (RT) genetic distance to the outgroup (all the Ty1 LTR RTs sequences of Asian arowana) and found that Asian arowana had a different LINE insertion time peak compared to African arowana and pirarucu, as well as an extra LTR insertion time peak which was close to its LINE insertion peak, indicating that Asian arowana had experienced a specific period (Figures 3D and 3E). To further figure out the function of the additional TEs insertion event, we investigated the TE coverage of all genes of these 3 species. In Asian arowana, we identified 1,261 genes located in TE-inserted regions, while this number in pirarucu and African arowana was only 464 and 73, respectively. The genes covered by TEs were concatenated together and had the same function (Figures 3F and S5). Functional enrichment analysis showed that these genes in Asian arowana were mainly related to olfactory transduction, NOD-like receptor signaling and phagosome pathways (Table S8, q-value<0.01). In summary, we found the genome of Asian arowana had gone through more changes due to the extra insertion of TEs, and also multiple gene families had expanded along with the copy and paste of TEs, which might be related to their adaptions to more variable environment after the first Gondwana split event than African arowana and pirarucu.

## *Dynamic Evolution of Gene Families*

Since we have observed a higher evolution rate in African arowana and more TEs insertion in Asian arowana, their effects on gene content were further evaluated by gene family analysis. We found the average gene family size of African arowana (1.38 gene per family) was less than Asian arowana and pirarucu (both 1.47 gene per

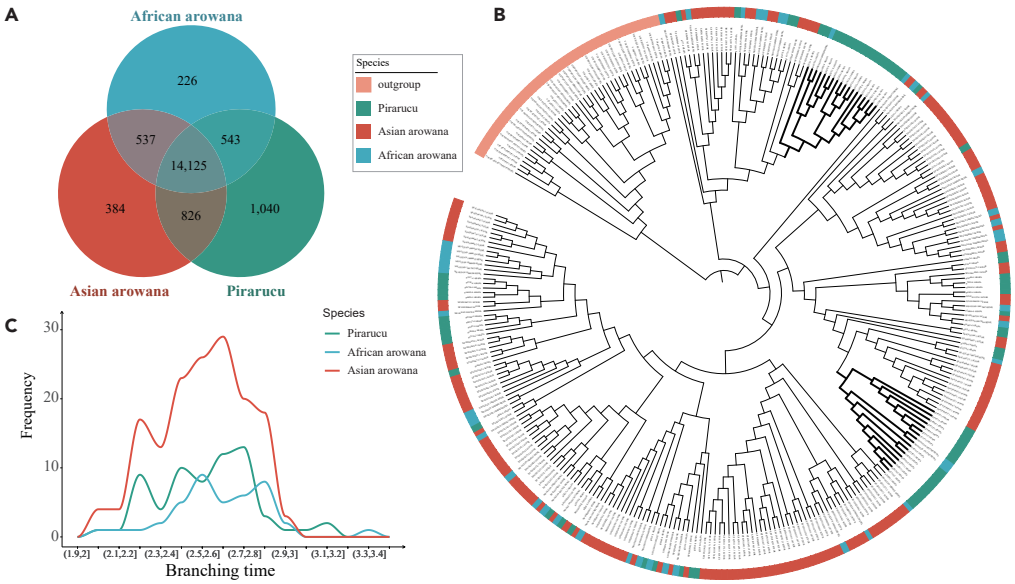


**Figure 4. Gene Family Dynamics of Three *Osteoglossidae* Fishes**

(A) The venn diagram represents the overlap relationship of three *Osteoglossidae* fishes' gene families.

(B) The gene tree of three *Osteoglossidae* fishes' *OR* genes in which the bold clades indicated two gene expansions of pirarucu.

(C) The insertion timeline of *OR* genes.

family), possibly indicating a higher evolutionary rate based on a published research (Chen et al., 2010). Overall, 14,125 gene families were shared by all these three species, and 1,040 gene families were unique to pirarucu (Figure 4A) which was more than that in Asian arowana (384) and African arowana (226). The unique gene families of Asian arowana were related to salivary secretion and olfactory transduction, whereas those of pirarucu were related to cell growth and death (necroptosis and apoptosis), and cellular community (tight junction, adherens junction, gap junction, and focal adhesion). Additionally, eight *UGT* (*K00699*) genes were found in the unique gene families of African arowana. *UGT* genes have been shown to play a critical role in many metabolism pathways such as ascorbate and aldarate metabolism, retinol metabolism, steroid hormone biosynthesis, and porphyrin & chlorophyll metabolism, which might be related to its special omnivorous diet character (Kakehi et al., 2015; Kawai et al., 2018) (Table S9, q-value<0.01).

We then detected 1,210, 424, and 829 expanded gene families in pirarucu, African arowana, and Asian arowana, respectively, (Figure S6). KEGG functional enrichment analysis of these expanded gene families showed that both pirarucu and Asian arowana had experienced significant expansion in 14 pathways including olfactory transduction, salivary secretion, cell adhesion molecules (CAMs) and NOD-like receptor signaling, which were not found in African arowana (Table S10, q-value<0.01). In contrast, the gene family contraction of African arowana (2,510) was more than Asian arowana (2,010) and pirarucu (1,151), which was related to olfactory transduction, tight junction, cellular senescence, TGF-beta signaling pathway (Table S11, q-value<0.01). More importantly, the expansion of *UGT* genes in African arowana further led to the expansion of several metabolic pathways.

## Possible Genetic Mechanisms Underpinning Diet Change of African Arowana

African arowana is an omnivore that has a wide range of preys including small benthic fishes, shrimps, plants, and insects (Adite et al., 2013; Monentcham et al., 2009). In contrast, its closely related species, pirarucu and Asian arowana, are predominantly dependent on fish preys (Natalia, 2004; Saint-Paul, 1986). In order to explore the genetic mechanisms of diet change in African arowana, we comprehensively examined the taste receptors of all tastes including sweet, umami, bitter, sour, and salty in these three genomes and found no significant differences in expansion or contraction (Table S11). The vertebrates have three kinds of odorant receptors including olfactory receptors (*ORs*), vomeronasal receptors *V1R* and *V2R* (Alioto and Ngai, 2005). Thus, then we carried out a comparative analysis of the odorant receptors of these three

genomes. The *V1R* genes and *V2R* genes in pirarucu, African arowana, and Asian arowana showed no obvious expansion (Table S12). However, we found that *OR* genes (*K04257*) were significantly contracted in African arowana (40) comparing with pirarucu (70) and Asian arowana (160). Through the gene tree of *ORs*, we further observed that Asian arowana had kept more gene copies in most clades of *OR*, while pirarucu had experienced contraction in several clades except for two clades (marked by bold clades, Figure 4B). In addition, in African arowana, almost all *OR* gene clades contained fewer members than that of Asian arowana and pirarucu. Estimation of the expanding time for *OR* genes showed that Asian arowana had gained much more *OR* gene copies during the whole timeline and had been through an extra insertion period, which can also be observed in pirarucu while only ancient *OR* expanding events were inferred in African arowana (Figure 4C). Given the results that the olfactory transduction pathway gene family underwent dynamic evolution in history and the expansion of *UGT* genes, we concluded that the change of *OR* genes and *UGT* genes might play a key role in the diet transition of African arowana.

## DISCUSSION

Continental drift leads to severe environmental change and geographical separation which would be the reason and driving force for differentiation and speciation (Chen et al., 2018; Dodd and Afzal Rafii, 2001). Phylogenetic relationships among those species which spread across different continents are of great interests for scientist from the establishment of plate tectonics (Casadevall et al., 2017; Sterrer, 1973; Wolfson, 1948). The evolutionary history of freshwater fish was also associated with the continental motion and discussed lively because of the ability to migrate across ocean for some species (Nakatani et al., 2011; Sparks and Smith, 2005). The *Osteoglossidae* species spread across all continents except Antarctica, serving as a typical subject to investigate the association between its speciation and continental drift. Here, we chose three representative *Osteoglossidae* species to investigate their divergence and revealed their genomics differences related to the continental motion.

We first assembled the genome of African arowana with advanced library-building and sequencing technologies because the genomes of Asian arowana and pirarucu were available. The stLFR technology was applied because of its cost-saving and convenience to get a better assembly without the need of multiple insertion libraries (Wang et al., 2018). The nanopore sequencing technology was applied to extend the genome continuity for its long reads. Also, we employed the power of Hi-C technology to link the scaffolds into pseudo-chromosomes. Eventually, we got the final African arowana genome with a better quality than recent researches about genome assemblies (Li et al., 2020; Xie et al., 2020). The genome sequences of African arowana provided important genetic resources for further researches.

The phylogenetic analysis in this study revealed a possible speciation track of *Osteoglossidae* species. Within 11 fishes' genome, we used conserved single-copy gene families which is reliable for phylogeny construction (Aguileta et al., 2008) to reveal the speciation history. By using MCMCtree and the calibration of published speciation time, we surprisingly found both the divergence time between African arowana & Asian arowana, and African arowana & pirarucu were consistent with the time of continental separation. The coincidences were supported by their geographical distribution and the fact that Africa is the biodiversity center of *Osteoglossiformes* and *Heterotidinae* (includes Africa arowana and pirarucu) fossil record found in North America. Together with the model of published Asian arowana's speciation history, we proposed a more complete model to reveal the speciation history of *Osteoglossidae*. Our model not only provides the possible speciation path of Asian arowana and pirarucu but will also guide the researches on paleontology in the future. Moreover, our results also hint a possibility of population genetic research to investigate their population history.

To reveal the evolutionary process they experienced, we focused on the genomic difference of three *Osteoglossidae* species. The faster evolutionary rate, less expansion and more contraction of gene families of African arowana were found. The association of evolutionary rate and dynamic changes of gene families was investigated previously, hinting a possible causality between African arowana's faster evolution rate and gene family contraction (Chen et al., 2010). We also found more class I TE insertions together with more genes covered by TE insertions which are concatenated in position and duplicated in function in Asian arowana genome. Published researches had reported the relation of genes and TEs in human genome and plant genome and had interpreted the effect of TEs on gene creation, gene evolution and genome rearrangement (Bennetzen, 2005; Nekrutenko and Li, 2001). Therefore, the evolutionary dynamics of gene families in African arowana and more TE insertions of Asian arowana probably play a key role in

their adaptive process to new environments. Moreover, we identified an expansion of SINE/5S elements in pirarucu whose function need to be further characterized (Figure S7).

We observed a significant difference in gene number of *OR* family among the three *Osteoglossidae* fishes, while the taste receptors, other odorant receptors *V1R* and *V2R* were conserved among them. Together with the expansion of *UGT* family in African arowana genome, we proposed a possible genetic mechanism underlying the diet change of African arowana. Diet change and the genomic evolution process had been investigated broadly (Perry et al., 2007; Schondube et al., 2001). Our research provides a case to investigate this phenomenon and a view to explain this process. However, when this change started and whether it happened on pirarucu is unknown because pirarucu experienced a similar contraction to African arowana in several clades of *OR* genes.

### Limitations of the Study

The data provided here are not sufficient to answer all questions we put forward. More researches will be required to conduct in the future such as the fossils evidence searching in Africa and South America. The impact of TEs insertion on new gene and gene expression regulation in Asian arowana also needs further study. The diet transition of African arowana and the inter-continental emigration of bonytongues should be transferable environments of freshwater fishes particularly for those living in the same period and similar environment with *Osteoglossidae*. Therefore, more evidences should be revealed in the future. Molecular biological experiments such as RNAi, gene knockout or genetic modification to verify the genetic mechanism underpinning the diet transition are also needed. Moreover, the additional *de novo* genomic researches and comparative genomic researches on *Osteoglossidae* and other *Osteoglossiformes* fish, which will help us to understand the evolution of this ancient teleost clade such as 10000 fish genome project (Fish10K) (Fan et al., 2020). The resequencing genomic and ancient genomic studies about these three *Osteoglossiformes* fishes were required to disclose the population structure, migration history, and genomic changes in their own genome along with the time.

### Resource Availability

#### *Lead Contact*

Further information and requests for resources should be directed to and will be fulfilled by the Lead Contact, Guangyi Fan (fanguangyi@genomics.cn).

#### *Materials Availability*

There is no resulting materials generated by this study.

#### *Data and Code Availability*

The accession numbers for the genome sequencing data, RNA sequencing data, and genome assembly reported in this paper are CNGBdb: CNP0001313 and NCBI: PRJNA665338.

## METHODS

All methods can be found in the accompanying Transparent Methods supplemental file.

## SUPPLEMENTAL INFORMATION

Supplemental Information can be found online at https://doi.org/10.1016/j.isci.2020.101662.

## ACKNOWLEDGMENTS

This work was supported by the National Key Research and Development Program of China (No. 2018YFD0900301-05). The work also received the technical support from China National GeneBank and Guangdong Provincial Key Laboratory of Genome Read and Write (No. 2017B030301011).

## AUTHOR CONTRIBUTIONS

Shijie Hao and Guangyi Fan conceived and designed the study. Mengqi Zhang and Yilin Wang performed sample collection and sequencing. Xiaoyun Huang performed assembly. Lingfeng Meng performed genome annotation and partial phylogenetic analysis. Kai Han performed pseudogene related analysis and partial phylogenetic analysis and designed the Figures 1 and 4. Shijie Hao performed partial genome

assembly, genome annotation and phylogenetic analysis, designed the Figures 2 and 3, wrote the manuscript. All other authors revised and read the manuscript.

## DECLARATION OF INTERESTS

The authors declare no competing interests.

Received: June 10, 2020
Revised: August 27, 2020
Accepted: October 7, 2020
Published: November 20, 2020

## REFERENCES

Adite, A., Ediye, M.M., Toko, I.I., Abou, Y., Imorou, R.S., and Sonon, S.P. (2017). Morphological and meristic characterization of the african bonytongue, Heterotis niloticus (cuvier, 1829), from lake hlan and sô river, southern Benin, west Africa: the need for habitat protection and species conservation. Int. J. Fish. Aquat. Res. *2*, 16–28.

Adite, A., Gbankoto, A., Toko, I.I., and Fiogbe, E.D. (2013). Diet breadth variation and trophic plasticity behavior of the African bonytongue Heterotis niloticus (Cuvier, 1829) in the Sô River-Lake Hlan aquatic system (Benin, West Africa): implications for species conservation and aquaculture development. Nat. Sci. *05*, 1219–1229.

Aguileta, G., Marthey, S., Chiapello, H., Lebrun, M.H., Rodolphe, F., Fournier, E., Gendrault-Jacquemard, A., and Giraud, T. (2008). Assessing the performance of single-copy genes for recovering robust phylogenies. Syst. Biol. *57*, 613–627.

Alioto, T.S., and Ngai, J. (2005). The odorant receptor repertoire of teleost fish. BMC Genomics *6*, 173.

Axelrod, H.R., Burgess, W.E., Pronek, N., and Walls, J.G. (1986). Dr. Axelrod's Atlas of Freshwater Aquarium Fishes (TFH Publications Neptune City).

Bennetzen, J.L. (2005). Transposable elements, gene creation and genome rearrangement in flowering plants. Curr. Opin. Genet. Dev. *15*, 621–627.

Betancur, R.R., Wiley, E.O., Arratia, G., Acero, A., Bailly, N., Miya, M., Lecointre, G., and Orti, G. (2017). Phylogenetic classification of bony fishes. BMC Evol. Biol. *17*, 162.

Bian, C., Hu, Y., Ravi, V., Kuznetsova, I.S., Shen, X., Mu, X., Sun, Y., You, X., Li, J., Li, X., et al. (2016). The Asian arowana (Scleropages formosus) genome provides new insights into the evolution of an early lineage of teleosts. Sci. Rep. *6*, 24501.

Casadevall, A., Freij, J.B., Hann-Soden, C., and Taylor, J. (2017). Continental drift and speciation of the cryptococcus neoformans and cryptococcus gattii species complexes. mSphere *2*, e00103-17.

Chen, F.C., Chen, C.J., Li, W.H., and Chuang, T.J. (2010). Gene family size conservation is a good indicator of evolutionary rates. Mol. Biol. Evol. *27*, 1750–1758.

Chen, J., Hao, Z., Guang, X., Zhao, C., Wang, P., Xue, L., Zhu, Q., Yang, L., Sheng, Y., Zhou, Y., et al. (2018). Liriodendron genome sheds light on angiosperm phylogeny and species–pair differentiation. Nat. Plants *5*, 18–25.

Cioffi, M.B., Rab, P., Ezaz, T., Bertollo, L.A.C., Lavoue, S., Oliveira, E.A., Sember, A., Molina, W.F., Souza, F.H.S., Majtanova, Z., et al. (2019). Deciphering the evolutionary history of arowana fishes (teleostei, Osteoglossiformes, Osteoglossidae): insight from comparative cytogenomics. Int. J. Mol. Sci. *20*, 4296.

Dodd, R.S., and Afzal Rafii, Z. (2001). Evolutionary genetics of mangroves: continental drift to recent climate change. Trees *16*, 80–86.

Du, K., Wuertz, S., Adolfi, M., Kneitz, S., Stock, M., Oliveira, M., Nobrega, R., Ormanns, J., Kloas, W., Feron, R., et al. (2019). The genome of the arapaima (Arapaima gigas) provides insights into gigantism, fast growth and chromosomal sex determination system. Sci. Rep. *9*, 5293.

Fan, G., Song, Y., Yang, L., Huang, X., Zhang, S., Zhang, M., Yang, X., Chang, Y., Zhang, H., Li, Y., et al. (2020). Initial data release and announcement of the 10,000 fish genomes project (Fish10K). Gigascience *9*, giaa080.

Gallant, J.R., Losilla, M., Tomlinson, C., and Warren, W.C. (2017). The genome and adult somatic transcriptome of the mormyrid electric fish paramormyrops kingsleyae. Genome Biol. Evol. *9*, 3525–3530.

Glasauer, S.M., and Neuhauss, S.C. (2014). Whole-genome duplication in teleost fishes and its evolutionary consequences. Mol. Genet. Genomics *289*, 1045–1060.

Guo-Qing, L., and Wilson, M.V.H. (1996). The discovery of Heterotidinae (teleostei: Osteoglossidae) from the Paleocene paskapoo formation of alberta, Canada. J. Vertebr. Paleontol. *16*, 198–209.

Hilton, E.J. (2001). Tongue bite apparatus of osteoglossomorph fishes: variation of a character complex. Copeia *2*, 372–381.

Hilton, E.J. (2003). Comparative osteology and phylogenetic systematics of fossil and living bony-tongue fishes (Actinopterygii, Teleostei, Osteoglossomorpha). Zool. J. Linn. Soc. *137*, 1–100.

Kakehi, M., Ikenaka, Y., Nakayama, S.M., Kawai, Y.K., Watanabe, K.P., Mizukawa, H., Nomiyama, K., Tanabe, S., and Ishizuka, M. (2015). Uridine diphosphate-glucuronosyltransferase (UGT) xenobiotic metabolizing activity and genetic evolution in pinniped species. Toxicol. Sci. *147*, 360–369.

Kawai, Y.K., Ikenaka, Y., Ishizuka, M., and Kubota, A. (2018). The evolution of UDP-glycosyl/glucuronosyltransferase 1E (UGET1E) genes in bird lineages is linked to feeding habits but UGT2 genes is not. PLoS One *13*, e0205266.

Kumazawa, Y., and Nishida, M. (2000). Molecular phylogeny of osteoglossoids: a new model for gondwanian origin and plate tectonic transportation of the asian arowana. Mol. Biol. Evol. *17*, 1869–1878.

Lavoue, S. (2016). Was Gondwanan breakup the cause of the intercontinental distribution of Osteoglossiformes? A time-calibrated phylogenetic test combining molecular, morphological, and paleontological evidence. Mol. Phylogenet. Evol. *99*, 34–43.

Lavoue, S., and Sullivan, J.P. (2004). Simultaneous analysis of five molecular markers provides a well-supported phylogenetic hypothesis for the living bony-tongue fishes (Osteoglossomorpha: teleostei). Mol. Phylogenet. Evol. *33*, 171–185.

Li, F., Bian, L., Ge, J., Han, F., Zhihong, L., Xuming, L., Yongsheng, L., Zhishu, L., Huilai, S., Liu, C., et al. (2020). Chromosome-level genome assembly of the East Asian common octopus (Octopus sinensis) using PacBio sequencing and Hi-C technology. Mol. Ecol. Resour. https://doi.org/10.1111/1755-0998.13216.

Meng, G., Li, Y., Yang, C., and Liu, S. (2019). MitoZ: a toolkit for animal mitochondrial genome assembly, annotation and visualization. Nucleic Acids Res. *47*, e63.

Monentcham, S.-E., Kouam, J., Pouomogne, V., and Kestemont, P. (2009). Biology and prospect for aquaculture of African bonytongue, Heterotis niloticus (Cuvier, 1829): a review. Aquaculture *289*, 191–198.

Mu, X.-d., Song, H.-m., Wang, X.-j., Yang, Y.-x., Luo, D., Gu, D.-e., Luo, J.-r., and Hu, Y.-c. (2012). Genetic variability of the Asian arowana, Scleropages formosus, based on mitochondrial DNA genes. Biochem. Syst. Ecol. *44*, 141–148.

Nakatani, M., Miya, M., Mabuchi, K., Saitoh, K., and Nishida, M. (2011). Evolutionary history of Otophysi (Teleostei) a major clade of the modern

freshwater fishes Pangaean origin and Mesozoic radiation. BMC Evol. Biol. *11*, 1–25.

Natalia, Y. (2004). Characterization of digestive enzymes in a carnivorous ornamental fish, the Asian bony tongue Scleropages formosus (Osteoglossidae). Aquaculture *233*, 305–320.

Nekrutenko, A., and Li, W.-H. (2001). Transposable elements are found in a large number of human protein-coding genes. Trends Genet. *17*, 619–621.

Núñez, J., Chu-Koo, F., Berland, M., Arévalo, L., Ribeyro, O., Duponchelle, F., and Renno, J.F. (2011). Reproductive success and fry production of the paiche or pirarucu, Arapaima gigas (Schinz), in the region of Iquitos. Perú. Aquac. Res. *42*, 815–822.

Oliveira, E.A., Bertollo, L.A.C., Rab, P., Ezaz, T., Yano, C.F., Hatanaka, T., Jegede, O.I., Tanomtong, A., Liehr, T., Sember, A., et al. (2019). Cytogenetics, genomics and biodiversity of the south American and african arapaimidae fish family (teleostei, Osteoglossiformes). PLoS One *14*, e0214225.

Perry, G.H., Dominy, N.J., Claw, K.G., Lee, A.S., Fiegler, H., Redon, R., Werner, J., Villanea, F.A., Mountain, J.L., Misra, R., et al. (2007). Diet and the evolution of human amylase gene copy number variation. Nat. Genet. *39*, 1256–1260.

Rafferty, J.P. (2010). Plate Tectonics, Volcanoes, and Earthquakes (Rosen Education Service).

Rogers, J.J.W., and Santosh, M. (2004). Continents and Supercontinents (Oxford University Press).

Saint-Paul, U. (1986). Potential for aquaculture of south american freshwater fishes: a review. Aquaculture *54*, 205–240.

Schondube, J.E., Herrera, M.L., and Martinez del Rio, C. (2001). Diet and the evolution of digestion and renal function in phyllostomid bats. Zoology (Jena) *104*, 59–73.

Scott, D.B.C., and Fuller, J.D. (1976). The reproductive biology of Scleropages formosus (Müller & Schlegel) (Osteoglossomorpha, Osteoglossidae) in Malaya, and the morphology of its pituitary gland. Fish Biol. *8*, 45–53.

Simao, F.A., Waterhouse, R.M., Ioannidis, P., Kriventseva, E.V., and Zdobnov, E.M. (2015). BUSCO: assessing genome assembly and annotation completeness with single-copy orthologs. Bioinformatics *31*, 3210–3212.

Sparks, J., and Smith, W. (2005). Freshwater fishes, dispersal ability, and nonevidence: "gondwana life rafts" to the rescue. Syst. Biol. *54*, 158–165.

Sterrer, W. (1973). Plate tectonics as a mechanism for dispersal and speciation in interstitial sand fauna. Neth. J. Sea Res. *7*, 200–222.

Tang, P.Y., Sivananthan, J., Pillay, S.O., and Muniandy, S. (2004). Genetic structure and biogeography of asian arowana (scleropages formosus) determined by microsatellite and mitochondrial DNA analysis. Asian Fish. Sci. *17*, 81–92.

Vialle, R.A., de Souza, J.E.S., Lopes, K.P., Teixeira, D.G., Alves Sobrinho, P.A., Ribeiro-Dos-Santos, A.M., Furtado, C., Sakamoto, T., Oliveira Silva, F.A., Herculano Correa de Oliveira, E., et al. (2018). Whole genome sequencing of the pirarucu (Arapaima gigas) supports independent emergence of major teleost clades. Genome Biol. Evol. *10*, 2366–2379.

Wang, O., Chin, R., Cheng, X., Ka Wu, M., Mao, Q., Tang, J., Sun, Y., Anderson, E., Lam, H.K., Chen, D., et al. (2018). Single tube bead-based DNA co-barcoding for cost effective and accurate sequencing, haplotyping, and assembly. BioRxiv. https://doi.org/10.1101/324392.

Wilson, M.V.H., and Murray, A.M. (2008). Osteoglossomorpha: phylogeny, biogeography, and fossil record and the significance of key African and Chinese fossil taxa. Geol. Soc. Lond. Spec. Publ. *295*, 185–219.

Wolfson, A. (1948). Bird migration and the concept of continental drift. Science *108*, 23–30.

Xie, J., Zhao, H., Li, K., Zhang, R., Jiang, Y., Wang, M., Guo, X., Yu, B., Kong, H., Jiao, Y., et al. (2020). A chromosome-scale reference genome of Aquilegia oxysepala var. kansuensis. Hortic. Res. *7*, 113.

Xu, M., Guo, L., Gu, S., Wang, O., Zhang, R., Fan, G., Xu, X., Deng, L., and Liu, X. (2019). TGS-GapCloser: fast and accurately passing through the Bermuda in large genome using error-prone third-generation long reads. bioRxiv. https://doi.org/10.1101/831248.

Yang, Z. (2007). Paml 4: phylogenetic analysis by maximum likelihood. Mol. Biol. Evol. *24*, 1586–1591.

**iScience, Volume *23***

## Supplemental Information

# African Arowana Genome Provides Insights on Ancient Teleost Evolution

**Shijie Hao, Kai Han, Lingfeng Meng, Xiaoyun Huang, Wei Cao, Chengcheng Shi, Mengqi Zhang, Yilin Wang, Qun Liu, Yaolei Zhang, Haixi Sun, Inge Seim, Xun Xu, Xin Liu, and Guangyi Fan**

# African arowana genome provides insights on ancient teleost evolution

Shijie Hao[1,2,7], Kai Han[2,7], Lingfeng Meng[1,2], Xiaoyun Huang[2], Wei Cao[3], Chengcheng Shi[1,2], Mengqi Zhang[2], Yilin Wang[2], Qun Liu[2], Yaolei Zhang[2,5], Haixi Sun[3], Inge Seim[6], Xun Xu[2,3], Xin Liu[2,3,4,*], Guangyi Fan[2,3,4,8,*].

[1]BGI Education Center, University of Chinese Academic of Sciences, Shenzhen 518083, China

[2]BGI-Qingqao, BGI-Shenzhen, Qingdao, 266555, China.

[3]BGI-Shenzhen, Shenzhen 518083, China.

[4]State Key Laboratory of Agricultural Genomics, BGI-Shenzhen, Shenzhen 518083, China.

[5]Department of Biotechnology and Biomedicine, Technical University of Denmark, Lyngby, 2800, Denmark.

[6]Comparative and Endocrine Biology Laboratory, Translational Research Institute-Institute of Health and Biomedical Innovation, School of Biomedical Sciences, Queensland University of Technology, Brisbane 4102, Queensland, Australia.

[7]These authors contributed equally.

[8]Lead Contact

[*]Correspondence: liuxin@genomics.cn (X.L.), fanguangyi@genomics.cn (G.F.).

## Transparent Methods

### Sample collection, library construction and genome sequencing

An individual African arowana fish from a seafood market at Xiamen, Fujian province, southeast China was collected and the muscle tissues were used for DNA extraction using the conventional salting-out method. The high molecular weight genomic DNA with an average length of 50 Kb was further used to construct a single tube Long Fragment Read (stLFR) library using the MGIEasy stLFR Library Prep kit (PN: 1000005622) according to the instructions(Wang et al., 2019). Hi-C library was constructed following the Wang's methods(Wang et al., 2019) with whole blood tissue of the same individual. The sequencing was conducted on a BGISEQ-500 platform with pair-end 100 bp read length. Besides, one nanopore library was also prepared according to the instructed protocol using the Oxford Nanopore SQK-LSK109 kit and sequenced on GridIon X5 platform.

### Genome survey

The *k*-mer frequencies within the clean stLFR reads were analyzed to estimate the major genome

characteristics. The occurrences of all 17-mers within both strands were counted using jellyfish v2.2.7(Marcais and Kingsford, 2011), and the genome size, heterozygosity as well as repeat content were calculated using GenomeScope (Vurture et al., 2017). The modeling distribution of 17-mer frequency demonstrated a peak at around 52, with 41,344,762,649 total number of *k*-mers. The estimated haploid genome size was 673.41Mb, of which 31% was inferred to be repeat, a low heterozygosity rate (0.13%) was detected while the *k-mer* distribution showed no apparent peak indicated heterozygosity in this genome.

**_De novo_ genome assembly**

Draft genome sequence was first assembled using Supernova v2.1.1(Weisenfeld et al., 2017) software and processed with one round of gap-closing using Gapcloser v1.12(Luo et al., 2012) with stLFR data. In this process, the stLFR reads were first pre-processed to be compatibly handled by supernova assembler, using the stLFR2Supernova pipeline (https://github.com/BGI-Qingdao/stlfr2supernova_pipeline). Then, we enhanced the draft assembly using TGS-GapCloser pipeline (Xu et al., 2019) based on the single molecular long reads.

Hi-C data were used to improve the connection integrity of the scaffolds. We first detected all valid pairs of reads using Hic-Pro v2.8.0(Servant et al., 2015) by mapping clean Hi-C reads to draft genome sequences, and the valid read pairs were extracted and aligned to the genome using Juicer v1.5(Durand et al., 2016b). Then the assembled fragments of DNA were ordered and oriented using 3D-DNA pipeline(Dudchenko et al., 2017) based on the Juicer Hi-C contacts ('merged_nodups.txt' file). Manual review and refinement were also performed by using Juicebox Assembly Tools v1.9.0(Durand et al., 2016a) to identify and remove the remaining assembly errors.

**Genome annotation**

We firstly detected and annotated the repetitive sequences in the genomes. For the annotation of TRFs, Tandem Repeats Finder v 4.04 program(Benson, 1999) was employed. The TEs were annotated by a combination of both *de novo* prediction and homology-based identification. Briefly, the genome sequences were *de novo* searched using LTR_Finder(Xu and Wang, 2007) and RepeatModeler(Smit et al., 2019) to find sequence elements with specific consensus models of putative interspersed repeats. The non-redundant self-contained repeat library was then searched against the genome using RepeatMasker (http://www.repeatmasker.org/). In the homology-based

detection, the genome sequences were aligned to both the public Repbase 21.01 and transposable element protein database (included in the RepeatMasker package) to detect interspersed repeats. Evidences including the results of ab initio gene predictors and homologous gene models to proteins previously discovered in other sequenced genomes, as well as transcript sequences were integrated to make a comprehensive gene structure annotation. The Augustus (Stanke et al., 2006), GlimmerHMM (Majoros et al., 2004) and Genescan (Burge and Karlin, 1997) were applied for ab initio gene finding with best parameters trained for zebrafish and vertebrates. For homology-based prediction, nonredundant protein sequences from 5 species (*Oreochromis niloticus*, *Pundamilia nyererei*, *Maylandia zebra*, *Astatotilapia calliptera* and *Scleropages formosus*) were aligned against African arowana genome using GeneWise v2.4.1 program(Birney et al., 2004). Furthermore, transcript sequences were constructed based on the RNA-Seq alignment to the genome that generated by using HISAT v2.1.0(Kim et al., 2019), and candidate coding regions within the transcripts were further detected, in which ORFs with homology to known proteins were also identified via blast (against SwissProt database) and pfam searches, using TransDecoder v5.5.0 (https://transdecoder.github.io/). Final consensus gene models were produced by integrating those disparate sources of gene structure evidence using GLEAN software (Elsik et al., 2007). Total 24,146 genes, covering 96.8% vertebrate benchmarking universal single-copy orthologs (BUSCOs)(Waterhouse et al., 2018), were predicted in the African arowana genome with average length 14911.23 bp. The length distributions of mRNA, coding sequences, exon and intron were closely similar to that of related species.

Functional annotations of the predicted genes were performed by aligning protein sequences using BLAST to KEGG release 84.0, Swissprot release 201709, Trembl release 201709 and Clusters of Orthologous Groups (COGs) database. The results show that 21,609 (89.49%) protein-coding genes were assigned successfully to at least one well-modeled functional category.

We also scanned matches of the protein sequences against the genomes of *Osteoglossidae* species (Aian arowana, African arowana and pirarucu) and detected the possible pseudogenes separately using PseudoPipe(Zhang et al., 2006) annotation tool. Pseudogenes overlapping a location of coding genes as well as those classified as fragment match were further discarded from the final annotation.

**Evolutionary phylogeny of African arowana**

To reveal the phylogenetic relationships of African arowana and other bony fishes, gene set of

five *Clupeocephala* species (*Danio rerio*, *Salmo salar*, *Oryzias latipes*, *Gasterosteus aculeatus* and *Takifugu rubripes*), one *Elopomorpha* species (*Anguilla rostrate*) and three *Osteoglossomorpha* species (*Scleropages formosus*, *Paramormyrops kingsleyae* and *Arapaima gigas*), plus one species from *Lepisosteiformes* (*Lepisosteus oculatus*) as outgroup, were downloaded from NCBI and further used to detect gene clusters. We extract the longest transcript from unique genomic loci to eliminate redundant splicing, and retained coding sequences longer than 150 bp from each dataset to discard possibly unreliable gene predictions. We performed all-versus-all BLAST search for protein sequences of these 11 species and the resultant matches were sorted out for filtering redundant and segments, then the genes were further clustered into 23,654 families using hcluster_sg tool (https://sourceforge.net/p/treesoft/code/HEAD/tree/branches/lh3/). We performed multiple sequences alignment using MUSCLE v3.7 software(Edgar, 2004) for each single-copy gene cluster and further concatenated the alignments into super-matrix. Phylogenetic relationships of these species were inferred using MrBayes v3.1.2 (Ronquist et al., 2012) based on the fourfold degenerate site of the supergene. The divergence time of our target species were also determined using MCMCTree (Yang, 2007) with the public timelines from TimeTree (Kumar et al., 2017) as calibrations. Given the phylogenetic relationship and divergence time, we analyzed the changes in gene family size using CAFE v2.1(De Bie et al., 2006). We compared the gene pairs in the paralogous and orthologous families detected by using wgd v1.0.1 package (Zwaenepoel and Van de Peer, 2019), the distribution of synonymous mutation rate (*Ks*) was used as an indicator of the duplication and divergence event in three *Osteoglossidae* species (*Scleropages formosus*, *Arapaima gigas* and *Heterotis niloticus*).

**Evolutionary rate calculation**

The 355 11-speceis one-to-one gene families were firstly used to calculate evolutionary rate by using the PAML v4.4c software. For every gene families, the dN and dS of non-sportted gar genes of each lineage were extracted from the result files and used for further statistics. To perform more extensive analysis, we identified one-to-one gene families among spotted gar and three *Osteoglossidae* fishes and calculated dN and dS with PAML too. Moreover, the conserved genome regions among three *Osteoglossidae* fishes and spotted gar were identified using MultiZ v1.0 software with genome alignments between every *Osteoglossidae* fish and spotted gar. Then, the genetic distances between *Osteoglossidae* fishes and spotted gar within the conserved regions were calculated using home-made python script and TN93 algorithm (**Script 1**). Finally, we

implemented syntenic analysis between Asian arowana & African arowana, Asian arowana itself and African arowana itself with Jcvi v0.8.12 toolkit.

**TE insertion timeline estimation**

To detect the insertion timeline of TEs within the 3 *Osteoglossidae* fish genomes, we firstly identified the transposable elements' conserved domains using DANTE pipeline (https://github.com/kavonrtep/dante). Protein sequences of RT (reverse transcriptase) domains from the most abundant TE types (here LINEs and LTR/Ty3s) were extracted for each of *Osteoglossidae* species. The sequences were further aligned, together with the same type of sequences from Asian arowana's LTR/Ty1 TEs, using MAFFT v7.453 (Katoh and Standley, 2013) program for each species. Then TE element trees were built based on the multiple sequences alignment using FastTree v2.1.10 (Price et al., 2010) and re-rooted on LTR/Ty1s to trace the evolutionary trajectory of LINEs or LTR/Ty3s. Concentration of branch length between terminal leaf and root node was calculated with a home-made python script and used to imply the explosion of TE element in each species.

**Genes and transposable elements phylogenetic trees construction**

We also investigated the evolutionary pathways of genes with similar function and repeat elements with the same class, within three *Osteoglossidae* fishes, based on the annotation results of RepeatMasker and KEGG (see Method). In this process, we used MAFFT program and FastTree software to perform the sequences alignment and tree building. All evolutionary trees were visualized using ggtree(Yu et al., 2017) package under R environment as well as the interactive online tool iTOL(Letunic and Bork, 2019). To screen and qualify gene trees with species-specific expanded clade, we traversed all nodes in a tree, by using an in-house python script (**script 2**) and ete3(Huerta-Cepas et al., 2016) module, to find out clade containing more than ten genes of which 80% were from the same species.

**In-house Scripts**

**Script 1. Calculate the genetic distance of conserved genome regions.**

```
#!/usr/bin/env python3

import os
import sys
```

```
from tn93 import tn93

class SEQ:
    def __init__(self, line):
        lst = line.split()
        self.source = lst[1]
        #self.name = source[0]
        #self.seqid = '.'.join(source[1:])
        self.start = int(lst[2]) + 1
        self.length = int(lst[3])
        self.strand = lst[4]
        source_length = int(lst[5])
        if self.strand == '-':
            self.end = source_length - self.start
            self.start = self.end - self.length + 1
        else:
            self.end = self.start + self.length - 1
        self.seq = lst[6].upper()

def calculate(sequences, score):
    target = sequences[0]
    length = len(target.seq)
    line = '{}:{}-{}{}'.format(target.source, target.start,
            target.end, target.strand)
    line += '\t{}\t{}'.format(length, score)
    for index, seq in enumerate(sequences[1:]):
        dist = tn93(target.seq, seq.seq, length,
                matchMode=3, min_overlap=length // 4)
        query = '{}:{}-{}{}:{:5f}'.format(seq.source, seq.start,
                seq.end, seq.strand, dist)
        line += ('\t' + query)
    return line + '\n'

if __name__ == '__main__':

    sys.stdout.write('#target\talign_length\tscore\tquery:dist\n')
    sequences = []
    r = open(sys.argv[1])
    for line in r:
        if line.startswith('#'):
            continue
        if line.startswith('a score='):
            score = line.strip().split('=')[1]
        if line.startswith('s '):
            sequences.append(SEQ(line))
        if line.startswith('\n'):
            info = calculate(sequences, score)
            sys.stdout.write(info)
```

```
            sequences = []
    r.close()
```

**Scripts 2. Select expanded gene trees.**

```
#!/usr/bin/env python3

import os
os.environ['QT_QPA_PLATFORM'] = 'offscreen'
import sys
import glob
from ete3 import Tree, TreeStyle, NodeStyle
indir, outdir, threshold = sys.argv[1:]

def standard(leaf_names):
    if len(leaf_names) < 10:
        return False
    else:
        FZ_names = [i for i in leaf_names if i.startswith('NH_')]
        YZ_names = [i for i in leaf_names if i.startswith('XP_')]
        if any((len(x)/len(leaf_names) >= float(threshold)) for x in [FZ_names, YZ_names]):
            return True
        else:
            return False


tree_dirs = glob.glob(os.path.join(indir, 'K*'))
dirname = lambda x:os.path.basename(x)

tree_files = [[dirname(x), os.path.join(x, '{}.pep.tree'.format(dirname(x)))]
        for x in tree_dirs]

pass_trees = []
for geneID, tree_file in tree_files:
    try:
        tree = Tree(tree_file, format=0)
    except:
        sys.stderr.write('*** Parse Error: {}\n'.format(tree_file))
        continue
    tree.convert_to_ultrametric(strategy='cladogram')
    tree.ladderize()
    tag = False
    for node in tree.traverse('levelorder'):
        leaf_names = node.get_leaf_names()
        if not standard(leaf_names):
            continue
        tag = True
    if tag:
```

```
            pass_trees.append([geneID, tree])

if not os.path.exists(outdir):
    os.makedirs(outdir)

tree_style = TreeStyle()
tree_style.mode = 'c'
tree_style.scale = 120
tree_style.show_leaf_name = False
#tree_style.optimal_scale_level = 'full'
FZnode_style = NodeStyle()
FZnode_style['fgcolor'] = 'red'
FZnode_style['size'] = 20
FZnode_style['hz_line_width'] = 5
FZnode_style['vt_line_width'] = 5
YZnode_style = NodeStyle()
YZnode_style['fgcolor'] = 'blue'
YZnode_style['size'] = 20
YZnode_style['hz_line_width'] = 5
YZnode_style['vt_line_width'] = 5
internal_node = NodeStyle()
internal_node['size'] = 0
internal_node['hz_line_width'] = 5
internal_node['vt_line_width'] = 5

for geneID, tree in pass_trees:
    for node in tree.traverse():
        if node.is_leaf():
            if node.name.startswith('NH_'):
                node.set_style(FZnode_style)
            elif node.name.startswith('XP_'):
                node.set_style(YZnode_style)
        else:
            node.set_style(internal_node)
    tree.render(os.path.join(outdir, '{}.png'.format(geneID)), tree_style=tree_style)
```

Supplementary Figure 1. The Kmer analysis curve generated by GenomeScope (related to Figure 1).

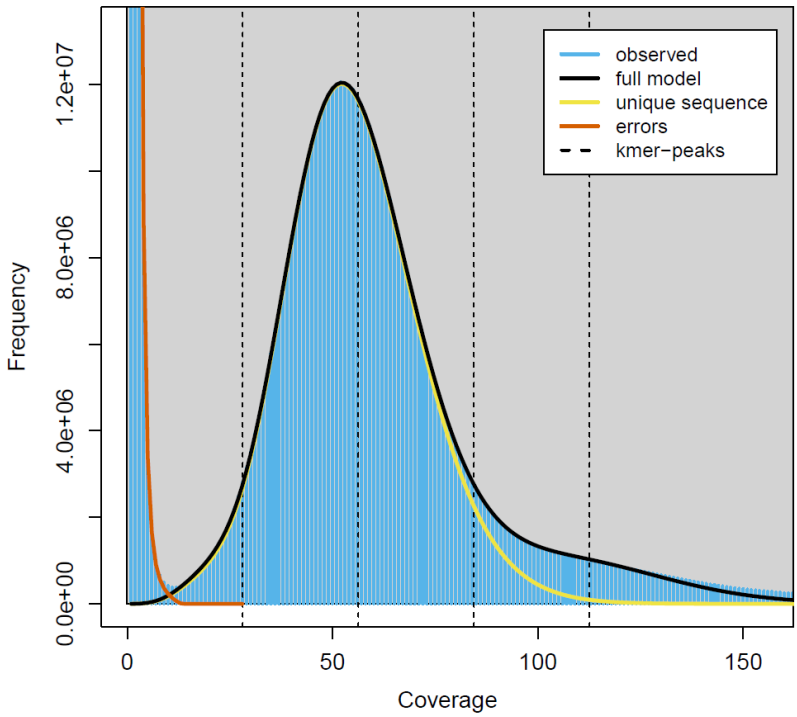


Supplementary Figure 2. The Hi-C assembly correlation heatmap (related to Figure 1).

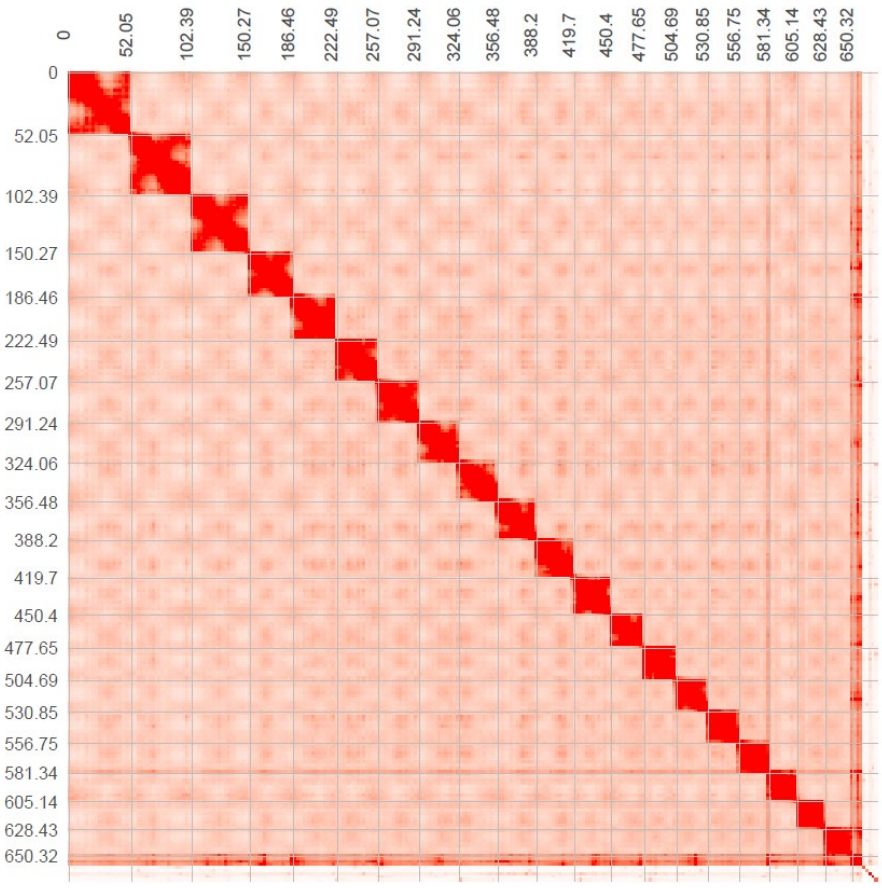


Supplementary Figure 3. The alignment spot plot of assembled and published mitochondrial genome of African arowana (related to Figure 1).

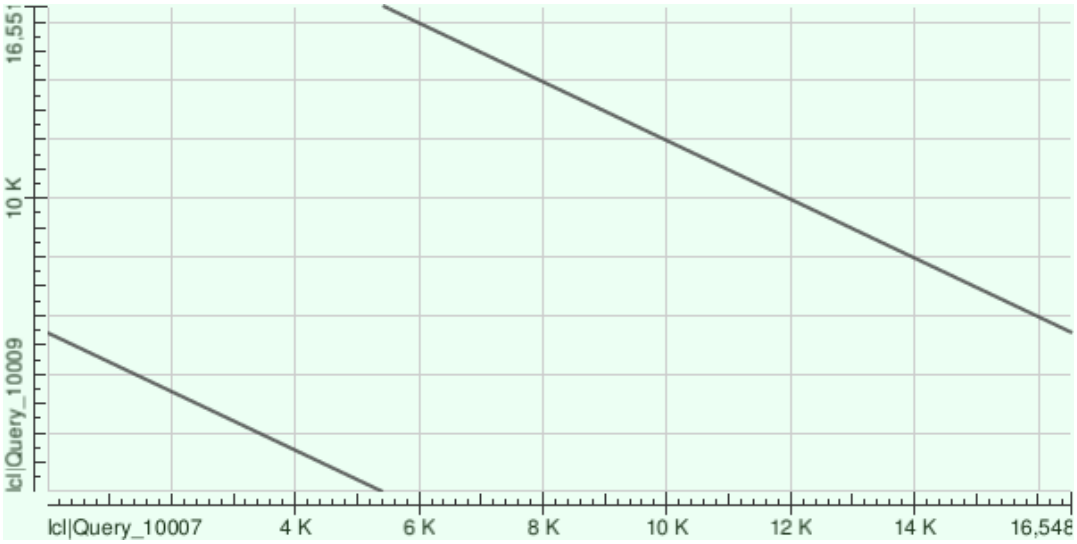


Supplementary Figure 4. The conserved regions genetic distance distribution (related to Figure 2).

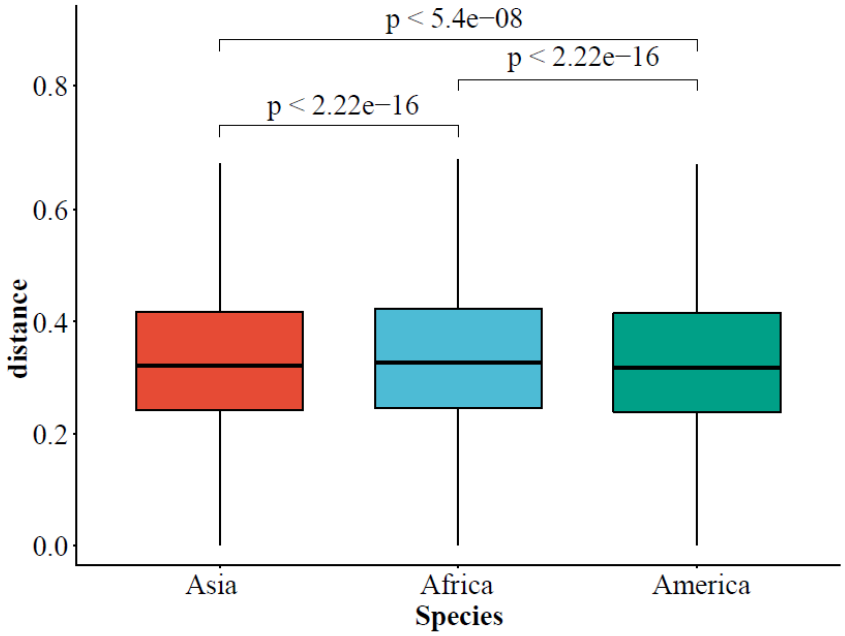


Supplementary Figure 5. The positional relationship of TEs and genes (related to Figure 3).

***K10492*** *(XP_029113551.1, XP_029113565.1, XP_029113577.1, XP_029113586.1, XP_029113603.1, XP_029113606.1, XP_029113677.1, XP_029113680.1)*

***K07418*** *(XP_029110465.1, XP_029110466.1, XP_029110467.1, XP_029110475.1, XP_029110477.1, XP_029110479.1, XP_029110482.1, XP_029110484.1, XP_029110485.1, XP_029110486.1, XP_029110487.1, XP_029110491.1, XP_029110494.1, XP_029110495.1, XP_029110668.1, XP_029110669.1, XP_029110672.1)*

***K10798*** *(XP_029111170.1, XP_029111360.1, XP_029111364.1, XP_029111367.1, XP_029111587.1, XP_029111590.1, XP_029111714.1)*

Supplementary Figure 6. Gene family expansion and contraction (related to Figure 4).

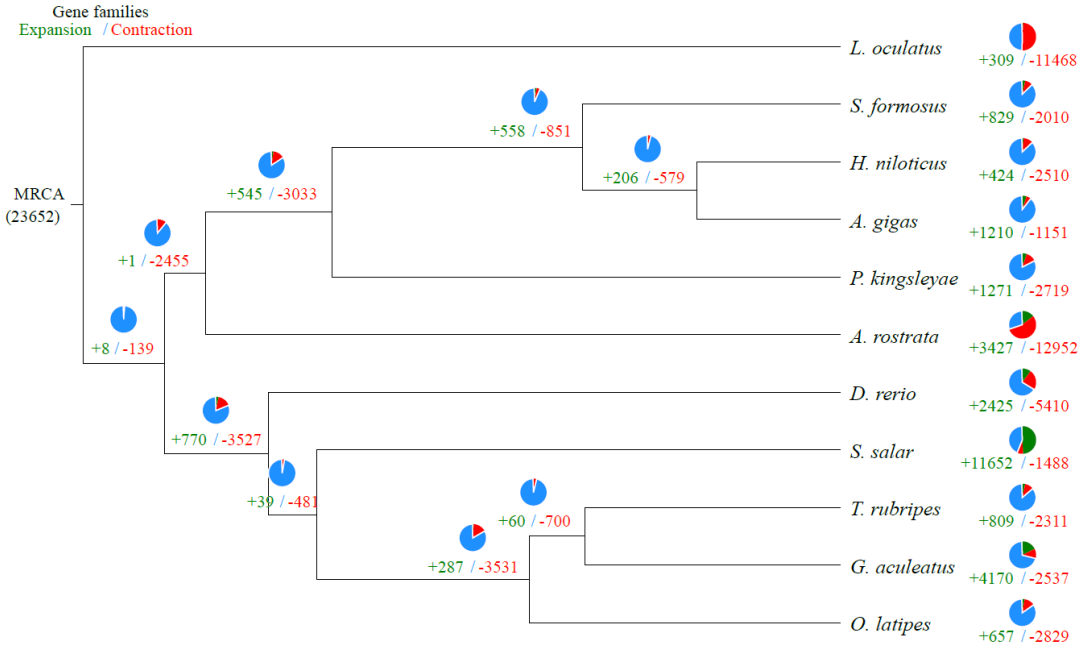


Supplementary Figure 7. 5S phylogenetic tree of three *Osteoglossidae* fishes (related to Figure 3).

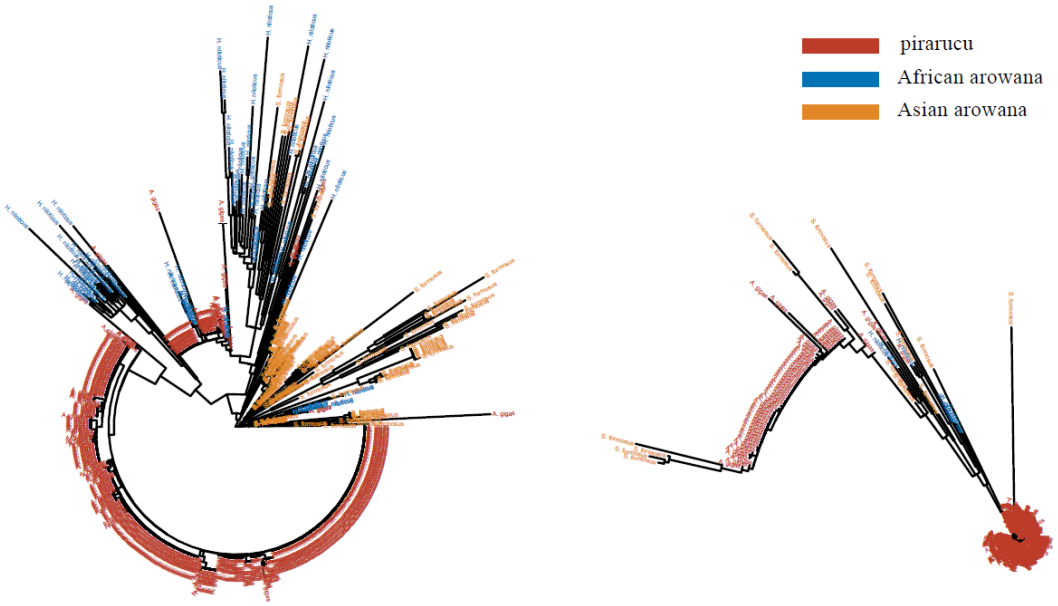

**Supplementary table 1. Sequenced data statistics (related to Figure 1).**

| Category | Bases number(bp) | genome coverage | read length |
|---|---|---|---|
| **stLFR** | 144,357,156,834 | 186.42 | PE 100+140 |
| **Nanopore** | 10,172,388,541 | 13.14 | Mean 20,695 |
| **Hi-C** | 21,234,895,000 | 27.42 | PE 100+100 |

**Supplementary table 2. Assemblies statistics (related to Figure 1).**

| #AssemblyName | #TotalScf | #ScfLen | #ScfN50 | #ScfN90 | #CtgNum | #CtgLen | #CtgN50 | #CtgMax | #GC(%) |
|---|---|---|---|---|---|---|---|---|---|
| **stLFR** | 4,244 | 669,728,546 | 9,615,753 | 2,219,485 | 20,530 | 663,211,256 | 75,203 | 520,346 | 43.04 |
| **Gapcloser** | 4,244 | 668,965,070 | 9,607,086 | 2,217,247 | 8,985 | 664,130,755 | 255,609 | 2,063,305 | 43.04 |
| **Gapcloser_hic** | 4,031 | 669,071,570 | 32,202,068 | 23,657,292 | 8,985 | 664,130,755 | 255,609 | 2,063,305 | 43.04 |
| **TGS_gapcloser** | 4,244 | 671,332,112 | 9,354,403 | 2,215,192 | 4,685 | 670,817,437 | 2,307,881 | 10,206,657 | 43.04 |
| **TGS_gapcloser_hic** | 3,995 | 671,456,612 | 32,427,226 | 23,803,277 | 4,685 | 670,817,437 | 2,307,881 | 10,206,657 | 43.04 |

**Supplementary table 3. Chromosome statistics (related to Figure 1).**

| Chromosome | Length | Gene num | Gene num per Mb |
|---|---|---|---|
| chr1 | 51,871,654 | 1,789 | 34.49 |
| chr2 | 49,976,607 | 1,704 | 34.10 |
| chr3 | 47,507,736 | 1,693 | 35.64 |
| chr4 | 36,097,016 | 1,096 | 30.36 |
| chr5 | 35,841,748 | 1,402 | 39.12 |
| chr6 | 34,505,377 | 1,317 | 38.17 |
| chr7 | 34,149,782 | 1,158 | 33.91 |
| chr8 | 32,770,312 | 1,234 | 37.66 |
| chr9 | 32,202,068 | 1,476 | 45.84 |
| chr10 | 31,542,738 | 1,291 | 40.93 |

| | | | |
|---|---|---|---|
| chr11 | 31,366,365 | 1,152 | 36.73 |
| chr12 | 30,527,933 | 1,199 | 39.28 |
| chr13 | 27,111,882 | 1,156 | 42.64 |
| chr14 | 27,037,882 | 963 | 35.62 |
| chr15 | 25,963,407 | 952 | 36.67 |
| chr16 | 25,831,899 | 937 | 36.27 |
| chr17 | 24,583,205 | 798 | 32.46 |
| chr18 | 23,657,292 | 707 | 29.89 |
| chr19 | 23,251,436 | 783 | 33.68 |
| chr20 | 21,895,334 | 666 | 30.42 |

**Supplementary table 4. BUSCO evaluation statistics (related to Figure 1).**

| | Complete(C) | Complete and single-copy(S) | Complete and duplicated(D) | Fragmented(F) | Missing(M) | Total |
|---|---|---|---|---|---|---|
| **Genome** | 2,522 | 2,303 | 219 | 33 | 31 | 2,586 |
| **Gene set** | 2,503 | 2,239 | 264 | 54 | 29 | 2,586 |

**Supplementary table 5. Gene orthologous statistics in public database (related to Figure 1).**

| Values | Total | Nr-Annotated | Swissprot-Annotated | KEGG-Annotated | TrEMBL-Annotated | Overall |
|---|---|---|---|---|---|---|
| **Number** | 24,146 | 21,553 | 20,915 | 19,504 | 21,597 | 21,621 |
| **Percentage** | 100% | 89.26% | 86.62% | 80.78% | 89.44% | 89.54% |

**Supplementary table 6. Fossil records used for divergence time calibration (related to Figure 1).**

| Species pairs | Calibration time |
|---|---|
| *Lepisosteus oculatus* vs *Anguilla rostrata* | 295-334 MYA |
| *Anguilla rostrate* vs *Heterotis niloticus* | 244-295 MYA |
| *Salmo salar* vs *Heterotis niloticus* | 231-287 MYA |

| | |
|---|---|
| *Oryzias latipes* vs *Danio rerio* | 206–252 MYA |

**Supplementary table 7. Repeat annotation statistics (related to Figure 3).**

| | | Repbase TEs | | De novo | | Combined TEs | | | |
|---|---|---|---|---|---|---|---|---|---|
| | | Length | percent | Length | percent | Length | percent | Length | percent |
| *H. niloticus* | **DNA** | 29,035,142 | 4.34 | 10,045,489 | 1.50 | 53,173,290 | 7.95 | 61,884,787 | 9.25 |
| | **LINE** | 17,099,871 | 2.56 | 14,416,154 | 2.15 | 31,437,295 | 4.70 | 37,093,168 | 5.54 |
| | **SINE** | 2,735,885 | 0.41 | 0 | 0.00 | 13,704,234 | 2.05 | 15,532,601 | 2.32 |
| | **LTR** | 4,909,599 | 0.73 | 2,355,009 | 0.35 | 18,023,858 | 2.69 | 20,631,561 | 3.08 |
| | **Other** | 43,744 | 0.01 | 0 | 0.00 | 0 | 0.00 | 43,744 | 0.01 |
| | **Unknown** | 0 | 0.00 | 0 | 0.00 | 17,467,985 | 2.61 | 17,467,985 | 2.61 |
| | **Total** | 48,975,430 | 7.32 | 26,801,920 | 4.01 | 119,546,525 | 17.87 | 125,391,143 | 18.74 |
| *S. formosus* | **DNA** | 42,415,841 | 5.41 | 175,473 | 0.02 | 61,270,356 | 7.81 | 87,560,384 | 11.16 |
| | **LINE** | 34,463,839 | 4.39 | 27,564,392 | 3.51 | 115,833,482 | 14.76 | 128,335,906 | 16.36 |
| | **SINE** | 10,836,721 | 1.38 | 0 | 0.00 | 5,937,128 | 0.76 | 16,323,535 | 2.08 |
| | **LTR** | 13,209,567 | 1.68 | 11,278,450 | 1.44 | 92,879,447 | 11.84 | 96,772,766 | 12.33 |
| | **Other** | 21,115 | 0.00 | 0 | 0.00 | 0 | 0.00 | 21,115 | 0.00 |
| | **Unknown** | 0 | 0.00 | 0 | 0.00 | 2,261,502 | 0.29 | 2,261,502 | 0.29 |
| | **Total** | 90,376,886 | 11.52 | 39,002,653 | 4.97 | 223,604,261 | 28.50 | 231,738,076 | 29.54 |
| *A. gigas* | **DNA** | 25,710,824 | 3.85 | 8,357,531 | 1.25 | 68,201,272 | 10.22 | 75,867,848 | 11.37 |
| | **LINE** | 7,978,164 | 1.20 | 5,907,459 | 0.89 | 16,704,546 | 2.50 | 22,111,177 | 3.31 |
| | **SINE** | 3,446,846 | 0.52 | 0 | 0.00 | 8,206,595 | 1.23 | 11,014,888 | 1.65 |
| | **LTR** | 6,016,996 | 0.90 | 3,889,739 | 0.58 | 26,970,615 | 4.04 | 30,740,524 | 4.61 |
| | **Other** | 16,768 | 0.00 | 129 | 0.00 | 0 | 0.00 | 16,897 | 0.00 |
| | **Unknown** | 0 | 0.00 | 0 | 0.00 | 10,605,989 | 1.59 | 10,605,989 | 1.59 |
| | **Total** | 37,937,812 | 5.68 | 18,144,719 | 2.72 | 113,468,148 | 17.00 | 121,187,526 | 18.16 |

**Supplementary Table 8. Transposable elements covered genes related pathways (related to Figure 4).**

| | #Pathway | CovergeBigThan0.9 | All-gene | Pvalue | Qvalue |
|---|---|---|---|---|---|
| *A. gigas* | NOD-like receptor signaling pathway | 56 | 404 | 1.31E-33 | 1.93E-31 |
| | Necroptosis | 47 | 349 | 1.03E-27 | 7.56E-26 |
| | Antigen processing and presentation | 30 | 151 | 4.58E-23 | 2.25E-21 |
| | Tight junction | 39 | 509 | 1.42E-14 | 5.21E-13 |
| | Salivary secretion | 26 | 279 | 5.36E-12 | 1.58E-10 |
| | Mitophagy - animal | 17 | 148 | 1.11E-09 | 2.71E-08 |
| | Endocytosis | 32 | 603 | 3.50E-08 | 7.35E-07 |
| | Longevity regulating pathway - multiple species | 15 | 160 | 1.64E-07 | 3.02E-06 |
| | Spliceosome | 16 | 254 | 1.24E-05 | 1.86E-04 |
| | Arginine and proline metabolism | 9 | 81 | 1.27E-05 | 1.86E-04 |
| | Estrogen signaling pathway | 16 | 271 | 2.75E-05 | 3.68E-04 |
| | PPAR signaling pathway | 9 | 132 | 0.000561226 | 6.05E-03 |
| | Protein processing in endoplasmic reticulum | 15 | 319 | 0.00057866 | 6.05E-03 |
| | Olfactory transduction | 11 | 191 | 0.000599972 | 6.05E-03 |
| | MAPK signaling pathway | 25 | 693 | 0.000617763 | 6.05E-03 |
| | Cardiac muscle contraction | 10 | 164 | 0.000678535 | 6.23E-03 |
| *H. niloticus* | NOD-like receptor signaling pathway | 12 | 288 | 4.24E-10 | 3.18E-08 |
| *S.formosus* | Olfactory transduction | 124 | 277 | 7.43E-81 | 1.49E-78 |
| | NOD-like receptor signaling pathway | 117 | 429 | 5.45E-49 | 5.45E-47 |
| | Phagosome | 84 | 327 | 3.28E-33 | 2.19E-31 |
| | Linoleic acid metabolism | 31 | 61 | 4.48E-23 | 2.24E-21 |
| | Ovarian steroidogenesis | 34 | 113 | 1.84E-16 | 7.36E-15 |
| | Arachidonic acid metabolism | 30 | 103 | 2.88E-14 | 9.61E-13 |

| | | | | | |
|---|---|---|---|---|---|
| | Salivary secretion | 46 | 254 | 1.25E-12 | 3.57E-11 |
| | Necroptosis | 51 | 319 | 1.03E-11 | 2.57E-10 |
| | Antigen processing and presentation | 30 | 138 | 1.02E-10 | 2.28E-09 |
| | Cytokine-cytokine receptor interaction | 50 | 402 | 9.60E-08 | 1.92E-06 |
| | Aminoacyl-tRNA biosynthesis | 23 | 118 | 1.30E-07 | 2.37E-06 |
| | Inflammatory mediator regulation of TRP channels | 33 | 237 | 1.20E-06 | 2.01E-05 |
| | alpha-Linolenic acid metabolism | 12 | 42 | 2.01E-06 | 2.97E-05 |
| | Apoptosis | 38 | 300 | 2.09E-06 | 2.97E-05 |
| | Neuroactive ligand-receptor interaction | 62 | 600 | 2.23E-06 | 2.97E-05 |
| | Serotonergic synapse | 31 | 226 | 3.45E-06 | 4.31E-05 |
| | TGF-beta signaling pathway | 32 | 245 | 6.89E-06 | 8.10E-05 |
| | Longevity regulating pathway - worm | 25 | 170 | 8.76E-06 | 9.73E-05 |
| | Gap junction | 26 | 189 | 1.96E-05 | 2.06E-04 |
| | Intestinal immune network for IgA production | 18 | 109 | 3.24E-05 | 3.24E-04 |
| | NF-kappa B signaling pathway | 27 | 224 | 0.00014015 | 1.33E-03 |
| | RIG-I-like receptor signaling pathway | 19 | 146 | 0.000504316 | 4.58E-03 |
| | Ether lipid metabolism | 14 | 92 | 0.000562398 | 4.89E-03 |
| | Mitophagy - animal | 18 | 140 | 0.000808824 | 6.74E-03 |

**Supplemental table 9. Unique gene families related pathways (related to Figure 4).**

| | #Pathway | unique_fam | All-gene | Pvalue | Qvalue |
|---|---|---|---|---|---|
| *A. gigas* | NOD-like receptor signaling pathway | 84 | 404 | 2.44E-20 | 5.09E-18 |
| | Necroptosis | 75 | 349 | 3.72E-19 | 3.89E-17 |
| | Phagosome | 67 | 319 | 1.03E-16 | 7.19E-15 |
| | Tight junction | 88 | 509 | 6.07E-16 | 3.17E-14 |
| | Cell adhesion molecules (CAMs) | 80 | 477 | 7.20E-14 | 3.01E-12 |

| | | | | | |
|---|---|---|---|---|---|
| | ECM-receptor interaction | 46 | 238 | 1.30E-10 | 4.52E-09 |
| | Mismatch repair | 18 | 50 | 2.20E-09 | 5.77E-08 |
| | Apoptosis | 56 | 349 | 2.21E-09 | 5.77E-08 |
| | Adherens junction | 43 | 257 | 4.64E-08 | 1.08E-06 |
| | Gap junction | 38 | 249 | 2.84E-06 | 5.93E-05 |
| | Focal adhesion | 65 | 533 | 4.41E-06 | 8.39E-05 |
| | Antigen processing and presentation | 26 | 151 | 1.19E-05 | 2.07E-04 |
| | Hematopoietic cell lineage | 26 | 153 | 1.51E-05 | 2.43E-04 |
| | Carbohydrate digestion and absorption | 15 | 83 | 0.000469753 | 7.01E-03 |
| *H. niloticus* | Ascorbate and aldarate metabolism | 9 | 27 | 8.02E-12 | 1.37E-09 |
| | Pentose and glucuronate interconversions | 9 | 35 | 1.12E-10 | 9.57E-09 |
| | Drug metabolism - cytochrome P450 | 9 | 44 | 1.03E-09 | 5.88E-08 |
| | Retinol metabolism | 10 | 67 | 3.08E-09 | 1.32E-07 |
| | Steroid hormone biosynthesis | 9 | 55 | 8.33E-09 | 2.85E-07 |
| | Porphyrin and chlorophyll metabolism | 8 | 46 | 3.48E-08 | 9.93E-07 |
| | Drug metabolism - other enzymes | 8 | 49 | 5.85E-08 | 1.25E-06 |
| | Metabolism of xenobiotics by cytochrome P450 | 8 | 49 | 5.85E-08 | 1.25E-06 |
| *S. formosus* | NOD-like receptor signaling pathway | 67 | 429 | 1.04E-37 | 2.11E-35 |
| | Salivary secretion | 30 | 254 | 5.43E-14 | 5.54E-12 |
| | Olfactory transduction | 26 | 277 | 4.69E-10 | 3.19E-08 |
| | Notch signaling pathway | 13 | 125 | 3.50E-06 | 1.79E-04 |
| | Oxidative phosphorylation | 14 | 174 | 2.91E-05 | 1.19E-03 |
| | Dorso-ventral axis formation | 11 | 113 | 3.67E-05 | 1.25E-03 |
| | Cell adhesion molecules (CAMs) | 23 | 416 | 4.70E-05 | 1.37E-03 |
| | PPAR signaling pathway | 11 | 124 | 8.61E-05 | 2.20E-03 |
| | Phenylalanine, tyrosine and tryptophan biosynthesis | 4 | 14 | 0.000186839 | 4.24E-03 |

| | | | | | |
|---|---|---|---|---|---|
| | Long-term potentiation | 12 | 171 | 0.000382786 | 7.81E-03 |
| | Phenylalanine metabolism | 5 | 30 | 0.000435588 | 8.08E-03 |

**Supplementary Table 10. The expanded gene families related pathways (related to Figure 4).**

| | #Pathway | Expanded gene number | All gene number | Pvalue | Qvalue |
|---|---|---|---|---|---|
| *A.gigas* | Cell adhesion molecules (CAMs) | 156 | 477 | 1.12E-22 | 2.58E-20 |
| | NOD-like receptor signaling pathway | 130 | 404 | 1.92E-18 | 2.21E-16 |
| | Olfactory transduction | 69 | 191 | 4.40E-13 | 3.37E-11 |
| | Salivary secretion | 89 | 279 | 7.97E-13 | 4.58E-11 |
| | Intestinal immune network for IgA production | 43 | 107 | 2.24E-10 | 8.79E-09 |
| | Antigen processing and presentation | 54 | 151 | 2.29E-10 | 8.79E-09 |
| | Tight junction | 128 | 509 | 1.17E-09 | 3.85E-08 |
| | Cardiac muscle contraction | 54 | 164 | 6.92E-09 | 1.99E-07 |
| | Necroptosis | 92 | 349 | 2.32E-08 | 5.92E-07 |
| | Phagosome | 85 | 319 | 4.65E-08 | 1.07E-06 |
| | Mismatch repair | 23 | 50 | 1.84E-07 | 3.86E-06 |
| | Insulin secretion | 61 | 213 | 2.47E-07 | 4.73E-06 |
| | Gap junction | 67 | 249 | 8.08E-07 | 1.43E-05 |
| | Adrenergic signaling in cardiomyocytes | 95 | 392 | 9.43E-07 | 1.55E-05 |
| | Carbohydrate digestion and absorption | 30 | 83 | 1.68E-06 | 2.58E-05 |
| | Protein digestion and absorption | 74 | 290 | 1.98E-06 | 2.85E-05 |
| | Estrogen signaling pathway | 66 | 271 | 3.43E-05 | 4.64E-04 |
| | Notch signaling pathway | 40 | 146 | 8.04E-05 | 1.03E-03 |
| | Proximal tubule bicarbonate reclamation | 19 | 55 | 2.58E-04 | 3.13E-03 |
| | Inflammatory mediator regulation of TRP channels | 57 | 243 | 3.23E-04 | 3.71E-03 |
| | Phototransduction - fly | 26 | 91 | 6.72E-04 | 7.36E-03 |

| | | | | | |
|---|---|---|---|---|---|
| *H.niloticus* | Drug metabolism - cytochrome P450 | 14 | 44 | 3.16E-08 | 6.13E-06 |
| | Ascorbate and aldarate metabolism | 10 | 27 | 6.03E-07 | 4.59E-05 |
| | Progesterone-mediated oocyte maturation | 26 | 167 | 7.10E-07 | 4.59E-05 |
| | Drug metabolism - other enzymes | 13 | 49 | 1.03E-06 | 5.02E-05 |
| | Arginine and proline metabolism | 16 | 81 | 4.33E-06 | 1.68E-04 |
| | Retinol metabolism | 14 | 67 | 8.61E-06 | 2.78E-04 |
| | Retrograde endocannabinoid signaling | 29 | 241 | 3.12E-05 | 8.64E-04 |
| | Metabolism of xenobiotics by cytochrome P450 | 11 | 49 | 3.90E-05 | 9.45E-04 |
| | Regulation of lipolysis in adipocytes | 19 | 134 | 8.09E-05 | 1.74E-03 |
| | Necroptosis | 29 | 259 | 1.15E-04 | 2.23E-03 |
| | Adrenergic signaling in cardiomyocytes | 34 | 336 | 2.26E-04 | 3.99E-03 |
| | Selenocompound metabolism | 7 | 26 | 3.06E-04 | 4.38E-03 |
| | Gap junction | 23 | 197 | 3.09E-04 | 4.38E-03 |
| | NOD-like receptor signaling pathway | 30 | 288 | 3.16E-04 | 4.38E-03 |
| | Pentose and glucuronate interconversions | 8 | 35 | 3.89E-04 | 5.03E-03 |
| | Adipocytokine signaling pathway | 18 | 140 | 4.26E-04 | 5.16E-03 |
| | Glucagon signaling pathway | 22 | 193 | 5.76E-04 | 6.26E-03 |
| | Longevity regulating pathway - multiple species | 16 | 120 | 5.81E-04 | 6.26E-03 |
| | Gastric acid secretion | 21 | 184 | 7.48E-04 | 7.64E-03 |
| | Bile secretion | 17 | 136 | 8.40E-04 | 8.15E-03 |
| | MAPK signaling pathway - fly | 22 | 200 | 9.31E-04 | 8.60E-03 |
| | Cholinergic synapse | 25 | 241 | 1.02E-03 | 9.01E-03 |
| | Protein processing in endoplasmic reticulum | 28 | 284 | 1.16E-03 | 9.80E-03 |
| *S.formosus* | Olfactory transduction | 174 | 277 | 5.53E-82 | 1.27E-79 |
| | Phagosome | 151 | 327 | 2.53E-47 | 2.90E-45 |
| | NOD-like receptor signaling pathway | 159 | 429 | 2.73E-35 | 2.09E-33 |

| | | | | |
|---|---|---|---|---|
| Cell adhesion molecules (CAMs) | 140 | 416 | 2.88E-26 | 1.66E-24 |
| Linoleic acid metabolism | 41 | 61 | 6.95E-22 | 3.20E-20 |
| Intestinal immune network for IgA production | 56 | 109 | 3.84E-21 | 1.47E-19 |
| Antigen processing and presentation | 60 | 138 | 5.59E-18 | 1.84E-16 |
| Salivary secretion | 80 | 254 | 8.82E-14 | 2.54E-12 |
| Hematopoietic cell lineage | 60 | 174 | 1.51E-12 | 3.85E-11 |
| Necroptosis | 90 | 319 | 3.00E-12 | 6.91E-11 |
| Arachidonic acid metabolism | 42 | 103 | 6.80E-12 | 1.42E-10 |
| Ovarian steroidogenesis | 44 | 113 | 1.40E-11 | 2.67E-10 |
| Complement and coagulation cascades | 59 | 186 | 1.12E-10 | 1.98E-09 |
| Cytokine-cytokine receptor interaction | 99 | 402 | 1.15E-09 | 1.90E-08 |
| Inflammatory mediator regulation of TRP channels | 67 | 237 | 1.60E-09 | 2.45E-08 |
| Phototransduction | 32 | 82 | 7.71E-09 | 1.11E-07 |
| TGF-beta signaling pathway | 66 | 245 | 1.73E-08 | 2.34E-07 |
| alpha-Linolenic acid metabolism | 18 | 42 | 2.96E-06 | 3.77E-05 |
| Vascular smooth muscle contraction | 63 | 263 | 3.11E-06 | 3.77E-05 |
| Gastric acid secretion | 48 | 183 | 3.30E-06 | 3.80E-05 |
| Aminoacyl-tRNA biosynthesis | 35 | 118 | 3.67E-06 | 4.02E-05 |
| Phototransduction - fly | 27 | 81 | 4.18E-06 | 4.37E-05 |
| NF-kappa B signaling pathway | 55 | 224 | 5.89E-06 | 5.89E-05 |
| Protein digestion and absorption | 57 | 239 | 1.03E-05 | 9.89E-05 |
| Mineral absorption | 23 | 67 | 1.22E-05 | 1.12E-04 |
| GnRH signaling pathway | 52 | 214 | 1.43E-05 | 1.26E-04 |
| Cellular senescence | 72 | 338 | 4.91E-05 | 4.18E-04 |
| Gap junction | 45 | 189 | 8.75E-05 | 7.18E-04 |
| RIG-I-like receptor signaling pathway | 37 | 146 | 9.20E-05 | 7.30E-04 |

| | | | | |
|---|---|---|---|---|
| Estrogen signaling pathway | 52 | 232 | 1.39E-04 | 1.06E-03 |
| Long-term potentiation | 40 | 171 | 3.10E-04 | 2.30E-03 |
| Apoptosis | 62 | 300 | 3.74E-04 | 2.69E-03 |
| Oxytocin signaling pathway | 69 | 347 | 5.70E-04 | 3.97E-03 |
| Bile secretion | 33 | 140 | 8.64E-04 | 5.84E-03 |
| Ether lipid metabolism | 24 | 92 | 9.52E-04 | 6.26E-03 |
| Apelin signaling pathway | 59 | 295 | 1.19E-03 | 7.41E-03 |
| Proximal tubule bicarbonate reclamation | 15 | 48 | 1.19E-03 | 7.41E-03 |
| Neurotrophin signaling pathway | 55 | 274 | 1.56E-03 | 9.21E-03 |
| Serotonergic synapse | 47 | 226 | 1.56E-03 | 9.21E-03 |

**Supplementary table 11. The contracted gene families of African arowana related pathways (related to Figure 4).**

| #Pathway | Bonytongue.Henil.contracted (757) | All-gene (19504) | Pvalue | Qvalue |
|---|---|---|---|---|
| **Olfactory transduction** | 30 | 150 | 1.04E-13 | 2E-11 |
| **Tight junction** | 33 | 372 | 9.48E-06 | 0.0008 |
| **Cellular senescence** | 27 | 278 | 1.22E-05 | 0.0008 |
| **TGF-beta signaling pathway** | 21 | 200 | 3.54E-05 | 0.0018 |
| **Intestinal immune network for IgA production** | 11 | 66 | 4.28E-05 | 0.0018 |
| **Cell adhesion molecules (CAMs)** | 27 | 305 | 6.23E-05 | 0.0022 |
| **Vitamin digestion and absorption** | 9 | 48 | 8.21E-05 | 0.0024 |
| **Cytokine-cytokine receptor interaction** | 27 | 313 | 9.66E-05 | 0.0025 |
| **Signaling pathways regulating pluripotency of stem cells** | 25 | 297 | 0.00025 | 0.0059 |

**Supplementary table 12. Taste receptors statistics (related to Figure 4).**

| | *A. gigas* | *H. niloticus* | *S. formosus* |
|---|---|---|---|

| | | | |
|---|---|---|---|
| **K04624_TIR1 (Umami)** | 4 | 4 | 4 |
| **K04626_TIR3 (Sweet&Umami)** | 3 | 2 | 3 |
| **K08474_TAS2R (Bitter)** | 3 | 4 | 2 |
| **K04990_PKD2L1 (Sour)** | 1 | 1 | 1 |
| **K04824_SCNN1A (Salty)** | 1 | 1 | 1 |

**Supplementary table 13. Odorant receptors statistics (related to Figure 4).**

| | *A. gigas* | *H. niloticus* | *S. formosus* |
|---|---|---|---|
| **K04257_OR** | 70 | 45 | 160 |
| **K04614_V1R** | 14 | 15 | 14 |
| **K04613_V2R** | 2 | 2 | 1 |

## Reference


Benson, G. (1999). Tandem repeats finder: a program to analyze DNA sequences. Nucleic Acids Res *27*, 573-580.

Birney, E., Clamp, M., and Durbin, R. (2004). GeneWise and Genomewise. Genome Res *14*, 988-995.

Burge, C., and Karlin, S. (1997). Prediction of complete gene structures in human genomic DNA. J Mol Biol *268*, 78-94.

De Bie, T., Cristianini, N., Demuth, J.P., and Hahn, M.W. (2006). CAFE: a computational tool for the study of gene family evolution. Bioinformatics *22*, 1269-1271.

Dudchenko, O., Batra, S.S., Omer, A.D., Nyquist, S.K., Hoeger, M., Durand, N.C., Shamim, M.S., Machol, I., Lander, E.S., Aiden, A.P*., et al.* (2017). De novo assembly of the Aedes aegypti genome using Hi-C yields chromosome-length scaffolds. Science *356*, 92-95.

Durand, N.C., Robinson, J.T., Shamim, M.S., Machol, I., Mesirov, J.P., Lander, E.S., and Aiden, E.L. (2016a). Juicebox Provides a Visualization System for Hi-C Contact Maps with Unlimited Zoom. Cell Syst *3*, 99-101.

Durand, N.C., Shamim, M.S., Machol, I., Rao, S.S., Huntley, M.H., Lander, E.S., and Aiden, E.L. (2016b). Juicer Provides a One-Click System for Analyzing Loop-Resolution Hi-C Experiments. Cell Syst *3*, 95-98.

Edgar, R.C. (2004). MUSCLE: multiple sequence alignment with high accuracy and high throughput. Nucleic Acids Res *32*, 1792-1797.

Elsik, C.G., Mackey, A.J., Reese, J.T., Milshina, N.V., Roos, D.S., and Weinstock, G.M. (2007). Creating a honey bee consensus gene set. Genome Biol *8*, R13. doi: 10.1186/gb-2007-8-1-r13

Huerta-Cepas, J., Serra, F., and Bork, P. (2016). ETE 3: Reconstruction, Analysis, and Visualization of Phylogenomic Data. Mol Biol Evol *33*, 1635-1638.

Katoh, K., and Standley, D.M. (2013). MAFFT multiple sequence alignment software version 7: improvements in performance and usability. Mol Biol Evol *30*, 772-780.

Kim, D., Paggi, J.M., Park, C., Bennett, C., and Salzberg, S.L. (2019). Graph-based genome alignment and genotyping with HISAT2 and HISAT-genotype. Nat Biotechnol *37*, 907-915.

Kumar, S., Stecher, G., Suleski, M., and Hedges, S.B. (2017). TimeTree: A Resource for Timelines, Timetrees, and Divergence Times. Mol Biol Evol *34*, 1812-1819.

Letunic, I., and Bork, P. (2019). Interactive Tree Of Life (iTOL) v4: recent updates and new developments. Nucleic Acids Res *47*, W256-W259.

Luo, R., Liu, B., Xie, Y., Li, Z., Huang, W., Yuan, J., He, G., Chen, Y., Pan, Q., Liu, Y*., et al.* (2012). SOAPdenovo2: an empirically improved memory-efficient short-read de novo assembler. Gigascience *1*, 18. doi: 10.1186/2047-217X-1-18

Majoros, W.H., Pertea, M., and Salzberg, S.L. (2004). TigrScan and GlimmerHMM: two open source ab initio eukaryotic gene-finders. Bioinformatics *20*, 2878-2879.

Marcais, G., and Kingsford, C. (2011). A fast, lock-free approach for efficient parallel counting of occurrences of k-mers. Bioinformatics *27*, 764-770.

Price, M.N., Dehal, P.S., and Arkin, A.P. (2010). FastTree 2--approximately maximum-likelihood trees for large alignments. PLoS One *5*, e9490. doi: 10.1371/journal.pone.0009490

Ronquist, F., Teslenko, M., van der Mark, P., Ayres, D.L., Darling, A., Hohna, S., Larget, B., Liu, L., Suchard, M.A., and Huelsenbeck, J.P. (2012). MrBayes 3.2: efficient Bayesian phylogenetic inference and model choice across a large model space. Syst Biol *61*, 539-542.

Servant, N., Varoquaux, N., Lajoie, B.R., Viara, E., Chen, C.J., Vert, J.P., Heard, E., Dekker, J., and Barillot, E. (2015). HiC-Pro: an optimized and flexible pipeline for Hi-C data processing. Genome Biol *16*, 259. doi: 10.1186/s13059-015-0831-x

Stanke, M., Keller, O., Gunduz, I., Hayes, A., Waack, S., and Morgenstern, B. (2006). AUGUSTUS: ab initio prediction of alternative transcripts. Nucleic Acids Res *34*, W435-439.

Vurture, G.W., Sedlazeck, F.J., Nattestad, M., Underwood, C.J., Fang, H., Gurtowski, J., and Schatz, M.C. (2017). GenomeScope: fast reference-free genome profiling from short reads. Bioinformatics *33*, 2202-2204.

Wang, O., Chin, R., Cheng, X., Wu, M.K.Y., Mao, Q., Tang, J., Sun, Y., Anderson, E., Lam, H.K., Chen, D.*, et al.* (2019). Efficient and unique cobarcoding of second-generation sequencing reads from long DNA molecules enabling cost-effective and accurate sequencing, haplotyping, and de novo assembly. Genome Res *29*, 798-808.

Waterhouse, R.M., Seppey, M., Simao, F.A., Manni, M., Ioannidis, P., Klioutchnikov, G., Kriventseva, E.V., and Zdobnov, E.M. (2018). BUSCO Applications from Quality Assessments to Gene Prediction and Phylogenomics. Mol Biol Evol *35*, 543-548.

Weisenfeld, N.I., Kumar, V., Shah, P., Church, D.M., and Jaffe, D.B. (2017). Direct determination of diploid genome sequences. Genome Res *27*, 757-767.

Xu, M., Guo, L., Gu, S., Wang, O., Zhang, R., Fan, G., Xu, X., Deng, L., and Liu, X. (2019). TGS-GapCloser: fast and accurately passing through the Bermuda in large genome using error-prone third-generation long reads. bioRxiv. doi: 10.1101/831248

Xu, Z., and Wang, H. (2007). LTR_FINDER: an efficient tool for the prediction of full-length LTR retrotransposons. Nucleic Acids Res *35*, W265-268.

Yang, Z. (2007). PAML 4: phylogenetic analysis by maximum likelihood. Mol Biol Evol *24*, 1586-1591.

Yu, G., Smith, D.K., Zhu, H., Guan, Y., Lam, T.T.-Y., and McInerny, G. (2017). ggtree: anrpackage for visualization and annotation of phylogenetic trees with their covariates and other associated data. Methods in Ecology and Evolution *8*, 28-36.

Zhang, Z., Carriero, N., Zheng, D., Karro, J., Harrison, P.M., and Gerstein, M. (2006). PseudoPipe: an automated pseudogene identification pipeline. Bioinformatics *22*, 1437-1439.

Zwaenepoel, A., and Van de Peer, Y. (2019). wgd-simple command line tools for the analysis of ancient whole-genome duplications. Bioinformatics *35*, 2153-2155.